NF1 MUTATION ANALYSIS IN A CHILD HOMOZYGOUS FOR *MLH1* MUTATION

A THESIS SUBMITTED TO

THE DEPARTMENT OF MOLECULAR BIOLOGY AND GENETICS

AND THE INSTITUTE OF ENGINEERING AND SCIENCE OF

BILKENT UNIVERSITY

IN PARTIAL FULFILLMENT OF THE REQUIREMENTS

FOR THE DEGREE OF MASTER OF SCIENCE

BY

HANI S. M. AL-OTAIBI

JULY 1999

I certify that I have read this thesis and that in my opinion it is fully adequate, in scope and in quality, as a thesis for the degree of Master of Science.

Assist. Prof. Marie D. Ricciardone

I certify that I have read this thesis and that in my opinion it is fully adequate, in scope and in quality, as a thesis for the degree of Master of Science.

Assist. Prof. Uğur B. Yavuzer

I certify that I have read this thesis and that in my opinion it is fully adequate, in scope and in quality, as a thesis for the degree of Master of Science.

Prof. Aslıhan Tolun

Approved for the Institute of Engineering and Science

Director of Institute of Engineering and Science
Prof. Dr. Mehmet Baray

ABSTRACT

NF1 MUTATION ANALYSIS IN A CHILD HOMOZYGOUS FOR *MLH1* MUTATION

Hani S. M. Al-Otaibi
M.S. in Molecular Biology and Genetics
Supervisor: Assist. Prof. Marie D. Ricciardone
July 1999, 93 Pages

Hereditary nonpolyposis colorectal cancer (HNPCC) is a common autosomal dominant disease characterized by an inherited predisposition to early onset colorectal cancer and an increased risk of certain other cancers. Cancer susceptibility is due to a heterozygous germ line mutation in one of five mismatch repair (MMR) genes, with the majority of mutations found in MLH1 and MSH2. This study focused on a child with a homozygous germ line mutation in MLH1 [C676T→Arg226Stop] inherited from consanguineous parents (Ricciardone et al., 1999). This child presented with neurofibromatosis type 1 and hematological malignancy, instead of the colorectal cancer phenotype usually seen in HNPCC individuals. This severe tumorigenic syndrome most likely resulted from a downstream mutation in the NF1 gene that could not be repaired due to complete absence of DNA MMR activity. To confirm this hypothesis and possibly clarify the genetic mechanism involved in this phenotype, exons in the functional domain of NF1 that contained mononucleotide or dinucleotide repeat sequences were analyzed by single strand conformation polymorphism (SSCP) and DNA sequence analysis for the presence of mutations.

SSCP analysis of the child's DNA identified altered mobility of NF1 exon 22. Subsequent DNA sequence analysis revealed a heterozygous C3721T transition mutation. TaqI restriction digestion of the exon fragment confirmed loss of the restriction site, thus, verifying the sequencing results. The C3721T mutation results in substitution of a stop codon for an arginine codon at position 1241. The resulting NF1 gene product is truncated at the beginning of the functional GTPase activation domain. A putative somatic mutation in the wild-type allele caused complete loss of neurofibromin function. The resulting impaired regulation of Ras•GTP signaling probably contributed to tumor development -- neurofibromatosis and hematological malignancy. This NF1 mutation was not present in the mother, father or sibling, indicating that this was a de novo mutation that occurred in early embryogenesis, most probably as a downstream consequence of constitutional MMR deficiency.

ÖZET

MLH1 MUTASYONU İÇİN HOMOZİGOT OLAN BİR ÇOCUKTA *NF1* MUTASYON ANALİZİ

Hani S. M. Al-Otaibi
Moleküler Biyoloji ve Genetik Yüksek Lisans
Tez Yöneticisi: Yardımcı Doçent Dr. Marie D. Ricciardone
Temmuz 1999, 93 Sayfa

Kalıtsal polipoz olmayan kolorektal kanser, erken yaşta ortaya çıkan, diğer kanser türlerinin görülme insidansını artıran ve otozomal dominant kalıtım özelliği gösteren bir hastalıktır. Kansere yatkınlık, çoğunluğu *MLH1* ve *MSH2* genlerinde olmak üzere, beş yanlış eşleşme DNA tamir genlerinden herhangi birinde olan heterozigot eşey hücresi mutasyonundan kaynaklanmaktadır. Bu çalışma, bir akraba evliliğinden doğan ve homozigot eşey hücresinde *MLH1* geni mutasyonu [C676T→Arg226Stop] taşıyan bir çocuk üzerine yoğunlaşmıştır. Bu çocukta, genellikle HNPCC bireylerinde görülen kolorektal kanser fenotipi yerine, nörofibromatoz tip 1 ve hematolojik malignite görülmektedir. Bu ciddi tümorijenik sendrom, büyük olasılıkla, DNA MMR aktivitesi olmadığı için *NF1* geninde bulunan bir mutasyonun tamir edilememesi sonucu gelişmiştir. Bu hipotezi doğrulamak ve bu fenotipin oluşmasını etkileyen genetik mekanizmaya açıklık getirmek amacıyla, mononükleotid ya da dinükleotid tekrar dizileri içeren *NF1*'in fonksiyonel bölgesinde bulunan eksonlar tek iplikçikli yapısal çeşitlilik (SSCP) analizi ve DNA dizi analizi kullanılarak mutasyon varlığı açısından incelenmiştir.

DNA'nın SSCP analizi sonucunda, *NF1* ekson 22'de farklılık tanımlanmış ve DNA dizi analizi sonucunda, bir heterozigot C3721T geçiş mutasyonu ortaya çıkarılmıştır. Ayrıca, *Taq*I restriksiyon enzim analizi ile, bu eksondaki restriksiyon bölgesinin kaybolduğu saptanarak sekans sonuçları doğrulanmıştır. C3721T mutasyonu, bir arjinin kodonunun bir stop kodonuna dönüşümüne yol açmakta ve elde edilen *NF1* gen ürünü, fonksiyonel GTPase aktivasyon bölgesini taşımamaktadır. Yabanıl aleldeki olası bir somatik mutasyon, nörofibromin fonksiyonunun tamamen kaybolmasına sebep olmuştur. Böylece bozulan Ras•GTP sinyal regülasyonu, büyük bir olasılıkla tümör oluşumuna -- nörofibromatoza ve hematolojik maligniteye neden olmuştur. *NF1* mutasyonunun anne, baba ve kardeşte olmayışı, bunun, erken embriyogenezde, büyük olasılıkla yapısal MMR eksikliğine bağlı olarak gelişen bir de novo mutasyonu olduğunu göstermektedir.

To My Family

ACKNOWLEDGEMENTS

First of all, I would like to express my gratitude to my supervisor, Assist. Prof. Marie D. Ricciardone, for her kindness, advice, encouragement and all she gave to me during my work. She taught me much, and I am thankful for knowing her.

Many thanks to Prof. Mehmet Öztürk for his valuable advice and encouragement. I would like also to thank all my teachers at Bilkent: Tayfun, Uğur, Işık, Rengül, Günay, David, Can, Cengiz and Ergün.

For the one who stayed beside me, who cheered me up through my bad times, special thanks to Neslihani. Her support was of a different kind and I am grateful to be with her.

Special thanks to Birsen, Hilal, Cemaliye and Gökçe for their assistance in the lab. They were there whenever I asked for help.

Many thanks to all my friends in the department: Gürol, Arzu, Tuba, Tolga Çagatay, Berna, Emre, Burcu, Esra, Aslı, Bilada, Gülayşe, Tolga Emre, Nuri, Abdullah, Lutfiye, Sevim, Füsun and Tülay for providing me a good atmosphere and for making me feel like home.

Thank you all.

TABLE OF CONTENTS

Page

LIST OF TABLES

Page

LIST OF FIGURES

Page

1. INTRODUCTION

1.1. Description of TF3 Kindred

TF3 is a large HNPCC kindred, which has been studied previously in our department (Ricciardone *et al.*, 1999). The pedigree meets the Amsterdam criteria (Lynch *et al.*, 1993) for HNPCC, which states that there should be (1) at least three relatives, one of whom is a first-degree relative of the other two, with histologically verified colorectal cancer; (2) at least two generations affected by colorectal cancer; and (3) at least one colorectal cancer diagnosed before the age of 50. In this pedigree (Figure 1.1), 11 family members in three generations are afflicted with colorectal cancer and nine family members had early onset of colorectal cancer. So, this pedigree is consistent with the dominant inheritance of cancer susceptibility gene.

A heterozygous C676T (Arg226Stop) mutation in *MLH1* exon 8 was found to segregate with the disease (Ricciardone *et al.*, 1999). The consanguineous marriage between III-5 and III-6, both afflicted with colorectal cancer and both heterozygous for the *MLH1* mutation, resulted in three offspring (IV-2, IV-3 and IV-4), who died at early age of leukemia or lymphoma. Two of the children (IV-3 and IV-4) displayed neurofibromatosis type 1 (NF1). Analysis of archival DNA samples revealed that both children were homozygous for the *MLH1* mutation.

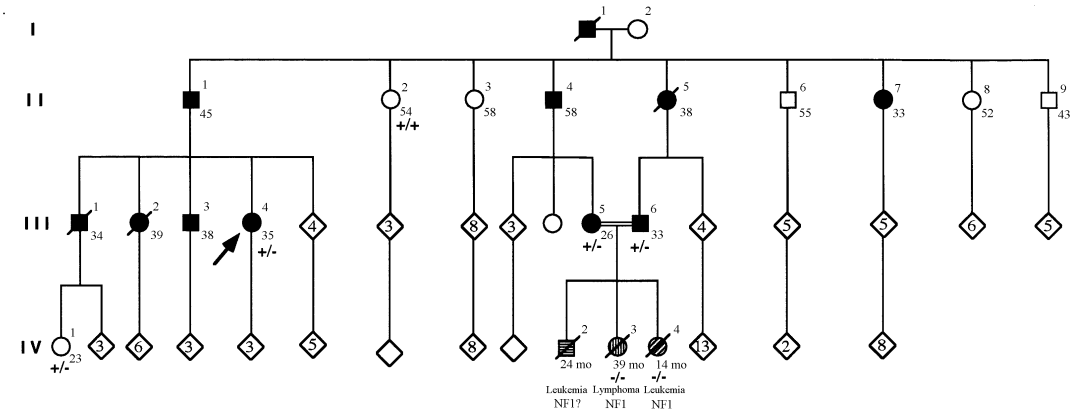

Figure 1.1. Pedigree of the HNPCC kindred. Filled symbols indicate colon cancer, shaded symbols indicate neurofibromatosis type 1. Numbers below symbols indicate age at diagnosis. (+/-): heterozygous *MLH1* mutation, (-/-): homozygous *MLH1* mutation (Ricciardone *et al.*, 1999).

Both children showed an unusual phenotype not previously observed in HNPCC kindreds -- neurofibromatosis type 1 and early onset hematological malignancy. A second, independent research study has identified an HNPCC kindred from North Africa with a similar characteristics (Wang *et al.*, 1999). We have hypothesized that the neurofibromatosis might be due to a downstream mutation in the *NF1* gene that resulted from a complete absence of DNA MMR activity as a consequence of the homozygous truncating mutation in *MLH1*. To confirm this hypothesis and possibly clarify the genetic mechanism involved in this phenotype, we plan to analyze mononucleotide and dinucleotide repeat sequences in the *NF1* coding regions for the presence of mutations.

1.2. Colorectal Cancer

Colorectal cancer is one of the leading causes of cancer mortality worldwide. About 50% of the Western population develops a colorectal polyp by the age of 70, and in about 1 in 10 of these individuals, malignancy develops (Kinzler and

Vogelstein, 1996). As a result, colorectal cancer is the second leading cause of cancer death in the United States and first when smoking related cancers are excluded (Parker *et al.*, 1996). Colorectal cancer develops as a result of the pathologic transformation of normal colonic epithelium to an adenomatous polyp and ultimately an invasive cancer. This transformation is a multistep process that occurs over decades and appears to require at least seven genetic events for completion (reviewed in Kinzler and Vogelstein, 1996).

1.2.1. Sporadic Colorectal Cancer

Over 90% of colorectal cancers are sporadic or nonfamilial (Moslein *et al.*, 1996). Colorectal cancer development is a multi-step process, driven by genetic alterations that confer a proliferative advantage on a specific cell. These genetic alterations occur in three classes of genes (reviewed in Gryfe *et al.*, 1997): (1) proto-oncogenes, which when mutated act to promote cell growth; (2) tumor suppressor genes, which when mutated fail to regulate cell proliferation; and (3) DNA repair genes, which when mutated fail to ensure the fidelity of DNA replication, leading to further mutations in proto-oncogenes and tumor suppressor genes.

Several epidemiological studies have linked lifestyle factors, especially diet, to the increased incidence of colorectal cancer. Lipids are thought to be among the critical dietary components because a higher rate of colorectal cancer has been associated with diets containing large amounts of red meat. Moreover, it has been shown that nonsteroidal anti-inflammatory drugs, that inhibit the cyclooxygenases that metabolize the lipid arachidonic acid, can prevent tumor formation and even

cause existing colorectal tumors to regress (reviewed in Kinzler and Vogelstein, 1996).

1.2.2. Familial / Hereditary Colorectal Cancer

Although cancer is a multi-step process, inheritance of a single mutant gene can markedly increase an individual's predisposition to colorectal cancer. Epidemiological studies suggested that 15% of colorectal cancers occur in dominantly inherited pattern (Kinzler and Vogelstein, 1996). Familial colorectal cancer syndromes include familial adenomatous polyposis (FAP) and hereditary non-polyposis colorectal cancer (HNPCC).

Familial adenomatous polyposis (FAP) is an autosomal dominantly inherited syndrome, characterized by development of hundreds of adenomatous colon polyps, some of which progress to cancer at an average age of 40 years (Kinzler and Vogelstein, 1996). The syndrome is caused by a germline mutation of the *APC* (adenomatous polyposis coli) gene (Kinzler *et al.*, 1991; Nishisho *et al.*, 1991; Groden *et al.*, 1991; Joslyn *et al.*, 1991) that has been mapped to chromosome position 5q21 (van der Luijt *et al.*, 1995). Patients with a germline mutation of *APC* do not necessarily develop colorectal cancer; however, they have a higher risk compared to the general population (Kinzler and Vogelstein, 1996). Tumor initiation requires somatic mutation and inactivation of the wild-type *APC* allele (Ichii *et al.*, 1992; Levy *et al.*, 1994) in agreement with Knudson's two-hit hypothesis for tumor suppressor genes (Knudson, 1993). FAP is almost completely penetrant but exhibits variable expression; some individuals exhibit polyps in the upper gastrointestinal

tract and others develop malignancies in organs outside the gastrointestinal tract. FAP has an estimated frequency of 1 in 10,000 in the general population (Gryfe *et al.*, 1997).

The precise biological function of the APC protein is not known. However, the APC protein can bind to and promote the degradation of β-catenin (Rubinfeld *et al.*, 1993). Mutations of *APC* result in the aberrant accumulation of β-catenin, which then binds T cell factor-4 (Tcf-4) causing transcription activation of unknown genes (Molenaar *et al.*, 1996; Behrens *et al.*, 1996). Recently, the *c-MYC* oncogene was identified as one of the downstream targets of β-catenin /Tcf (He *et al.*, 1998). The resulting overexpression of *c-MYC* could promote neoplastic growth.

Hereditary nonpolyposis colorectal cancer (HNPCC), also referred to as Lynch syndrome, is the second hereditary colorectal cancer syndrome. This syndrome is characterized by an autosomal dominant inherited predisposition to colorectal cancer that occurs at an early age (approximately 40-50 years old). Other cancers, such as endometrial, ovarian, small bowel, stomach, pancreas, ureter and renal pelvis may also be seen (Lynch *et al.*, 1996). Tumors isolated from HNPCC patients are distinguished by microsatellite instability (Aaltonen *et al.*, 1993; Thibodeau *et al.*, 1993) -- genome-wide insertions and deletions within simple tandem DNA repeats. About 70% of HNPCC kindreds inherit a germline mutation in one of the five genes involved in DNA mismatch repair (MMR), with the majority (95%) occurring in either *MLH1* or *MSH2* (Lynch and Smyrk, 1996).

1.3. Hereditary Non-Polyposis Colorectal Cancer (HNPCC)

Knowledge of genetics, coupled with a detailed family history, is necessary for diagnosis of HNPCC and genetic counseling. Until recently, a patient's cancer risk status could be evaluated with, at the most, a 50% level of confidence, based on the patient's HNPCC pedigree in accordance with the autosomal dominant mode of genetic transmission of the cancer trait. However, identification of the germline mutations responsible for HNPCC now enables the theoretical determination of genetic risk of cancer during embryogenesis (Lynch and Smyrk, 1996). The phenotypic penetrance of the deleterious genotype is approximately 85% to 90% (Lynch *et al.*, 1993; Lynch *et al.*, 1996).

1.3.1. Incidence of HNPCC

In an attempt to ascertain the true frequency of HNPCC, Mecklin *et al.* (1995), designed a nonselective, prospective, multicenter study that assessed family background and other risk factors of colorectal cancer over a 12-month period for all new colorectal cancer patients in 10 hospitals in Finland. They found three (0.7%) cases of verified HNPCC and seven (1.7%) cases of suspected HNPCC. This study revealed a lower frequency of HNPCC compared to previous investigations in Finland (Watson *et al.*, 1994). The lowest known estimate of HNPCC occurrence is 1%, which translates into 1500 new cases of HNPCC annually in the United States (Lynch *et al.*, 1996). Estimates of HNPCC incidence range as high as 5% or 7500 new occurrences of HNPCC in the United States each year (Lynch *et al.*, 1996). These estimates indicate that HNPCC poses a major public health problem.

1.3.2. Microsatellite instability in HNPCC

Microsatellite instability (MIN) is reflected as alterations in the patterns of polymorphic, short, tandem repeat segments (microsatellites) dispersed throughout the genome. Since the initial description in 1993 of microsatellite instability in HNPCC (Aaltonen *et al.*, 1993; Thibodeau *et al.*, 1993), MIN has been identified in a wide variety of human cancers, both familial and sporadic (Peltomaki *et al.*, 1993b; Thibodeau *et al.*, 1998; Moslein *et al.*, 1996; Dietmaier *et al.*, 1997; Tomlinson *et al.*, 1996). However, it has been difficult to derive a consensus concerning the role of MIN in human carcinogenesis. In the original descriptions of MIN in HNPCC, it was reported that MIN was associated with mutations in certain DNA repair genes (Leach *et al.*, 1993; Bronner *et al.*, 1994; Fishel *et al.*, 1993; Papadopoulos *et al.*, 1994; Nicolaides *et al.*, 1994). Therefore, the assumption is that MIN reflects an underlying genomic instability, resulting from inactivation of both alleles at a DNA repair gene locus.

Heterozygous individuals have apparently normal DNA mismatch repair activity (Parsons *et al.*, 1993). However, somatic mutation of the wild-type allele results in loss of this activity and accumulation of characteristic mutations, such as single base mispairs and length alterations in homopolymeric tracts (Parsons *et al.*, 1993). It has now been documented that the introduction of a wild type copy of a mismatch DNA repair gene into cell lines deficient for this gene can restore genomic stability of microsatellites (Umar *et al.*, 1997). This finding clearly indicates that mutations in mismatch DNA repair genes constitute the underlying molecular defect responsible for MIN.

Arzimanoglou *et al.* (1998) has reviewed the medical literature and concluded that MIN, associated with inherited mutations of the DNA mismatch repair genes, appears to characterize only the HNPCC / Muir-Torre family cancer syndromes and a subset of young sporadic colorectal carcinoma patients. MIN in non-HNPCC tumors generally is not associated with somatic mutations in DNA mismatch repair genes. Loci of individual chromosomes containing microsatellite markers demonstrating high MIN frequency may be linked to particular tumor types (tumor-specific MIN hot spots). MIN in tumors can be associated with early or late stages of tumor progression and also has been found in non-tumor tissues (Arzimanoglou *et al.*, 1998).

1.3.3. Molecular genetics of HNPCC

Molecular genetic studies have identified germline mutations in an increasingly large number of hereditary cancer syndromes, which has led to a good understanding of the molecular pathogenesis of the syndromes. Understanding of molecular pathogenesis of HNPCC has resulted from three related lines of investigation. The first was linkage analysis. Large kindreds from North America, Europe, and New Zealand were evaluated using microsatellite markers distributed throughout the genome. Tight linkage to either chromosome 2p16 or 3p21 was identified in individual families, providing unambiguous evidence that HNPCC was a simple Mendelian disease (Lindblom *et al.*, 1993; Peltomaki *et al.*, 1993a).

The second clue was found during attempts to demonstrate allelic losses with the 2p16 microsatellite markers linked with HNPCC susceptibility. Such losses are

often found to be associated with tumor suppressor loci. In HNPCC tumors, however, new microsatellite alleles, not found in the patient's normal cells, were observed instead of the expected allelic losses (Aaltonen *et al.*, 1993). Those new alleles were evident in every dinucleotide and trinucleotide repeat examined, suggesting a genome-wide instability of the replication or repair of simple repeated sequences.

The third clue was provided by investigators studying replication fidelity in unicellular organisms. These investigators recognized that the microsatellite instability observed in tumors was similar to that observed in bacteria harboring mutations in mismatch repair (MMR) genes such as *mutL* and *mutS* (Strand *et al.*, 1993; Wierdl *et al.*, 1996). Analogous experiments in yeast showed that microsatellites observed to be unstable in HNPCC patients were equally unstable in yeast with defective MMR genes and it was specifically hypothesized that HNPCC was caused by hereditary mutations of human homologues of *mutS* or *mutL* (Aaltonen *et al.*, 1993; Strand *et al.*, 1993).

These clues stimulated a search for human homologues likely to participate in MMR. That a *mutS* homologue might be involved in the form of HNPCC linked to chromosome 2 was suggested by the finding that one such homologue (*MSH2*) was located on chromosome 2p (Fishel *et al.*, 1993). Direct evidence that *MSH2* was involved in the disease was provided by the identification of germline mutations in HNPCC kindreds (Leach *et al.*, 1993). This observation was soon followed by the identification of mutations in the human *mutL* homologue *MLH1* (Bronner *et al.*, 1994; Papadopoulos *et al.*, 1994). Further search for other homologues uncovered

additional *mutL* homologues (*PMS1* and *PMS2*) that were found to be mutated in the germline of HNPCC kindreds (Nicolaides *et al.*, 1994). Later, two *mutS* homologues (*MSH3* and *MSH6*) were identified (Drummond *et al.*, 1995; Palombo *et al.*, 1995). Although somatic mutations in *MSH3* and *MSH6* were detected in HNPCC cancers (Risinger *et al.*, 1996; Akiyama *et al.*, 1997b), these genes were not mutated in the germline of typical HNPCC kindreds. However, a germline mutation has been found in an atypical HNPCC kindred (Akiyama *et al.*, 1997a). Mutations in two human MMR genes (*MSH2* and *MLH1*) account for the majority (>95%) of HNPCC kindreds (Papadopoulos and Lindblom, 1997).

1.3.4. DNA Mismatch Repair

DNA mismatch repair is a strand-specific process involving recognition of noncomplementary Watson-Crick base pairs (Lahue *et al.*, 1989). Mismatched base pairs in DNA can arise by several processes (reviewed in Kolodner, 1996). A significant source of mismatched bases is DNA replication errors. Occasionally, an incorrect nucleotide is incorporated into the DNA strand being synthesized. While the majority of these misincorporations are excised by the DNA polymerase proofreading 3'-5' exonuclease, approximately 1 in 10^9 errors remain. The DNA mismatch repair system can repair approximately 99.5% of the mutations that escape proofreading, thus, decreasing the error rate to 1 in 10^{12} base pairs (Schaaper, 1993; Lahue *et al.*, 1989). In this case, the correct base is located in the parental strand of the newly replicated DNA and correction of the mismatch helps maintain the fidelity of the genetic information. DNA polymerase slippage, another source of errors, usually occurs during replication of homopolymeric nucleotide tracts and results in

small insertions or deletions (Trinh and Sinden, 1991). A third source of mismatched nucleotides is genetic recombination between two DNA sequences that results in a heteroduplex sequence (reviewed in Fishel, 1998).

1.3.4.1. DNA Mismatch Repair in Prokaryotes

The most extensively characterized mismatch repair system is the *Escherichia coli* MutHLS system, which repairs a broad spectrum of mispaired bases and has been reconstituted with purified enzymes (Lahue *et al.*, 1989; Kolodner, 1996). The MutHLS repair pathway is uniquely suited to repair DNA replication errors (Modrich, 1991; Modrich, 1994; reviewed in Kolodner, 1995). Normally, DNA in *E. coli* is methylated at GATC sites by the Dam methylase. However, after DNA replication the daughter strand is transiently unmethylated. The MutHLS system utilizes this modification asymmetry to direct the repair to the unmethylated strand via the activity and involvement of several proteins.

Repair is initiated by the recognition and binding of MutS to a mismatched DNA base pair. MutL subsequently binds to MutS and activates MutH, which then nicks the unmethylated strand of DNA immediately 5' to the guanine residue of a hemi-methylated GATC site (Figure 1.2). The incised strand is then displaced by DNA helicase II and excised from the nick to the mispaired base by one of the single-stranded DNA exonucleases (Exonuclease I [3' exonuclease activity], Exonuclease VII [both 3' and 5' exonuclease activities] or RecJ exonuclease [5' exonuclease activity]) depending on whether the nicked is 5' or 3' to the mispair. The DNA strand is resynthesized by DNA polymerase III, with the participation of

single-strand DNA-binding proteins and DNA ligase (reviewed in Kolodner, 1996; Eshleman *et al.*, 1996).

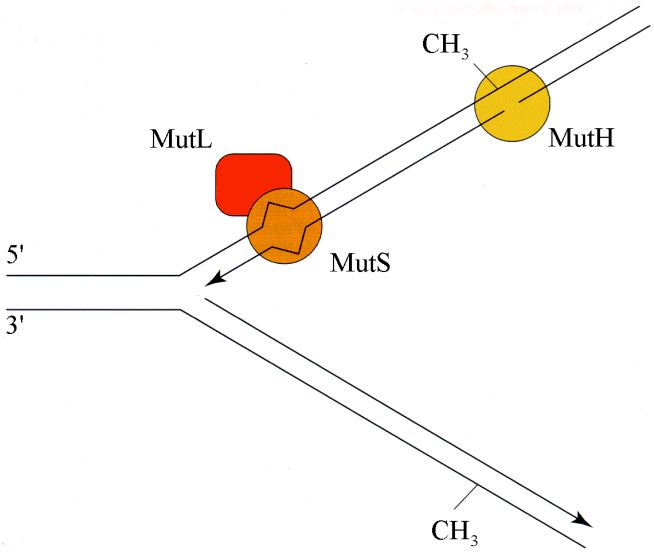

Figure 1.2. *E. coli* MutHLS DNA mismatch repair system at replication fork. Repair is initiated when MutS recognizes and binds the mismatch. Subsequently, MutL binds MutS and activates MutH, which then nicks the unmethylated strand of DNA at hemimethylated GATC sites. The unmethylated strand is then excised from the nick to the mispair. A new DNA strand is synthesized in the resulting gap (Kolodner, 1996).

1.3.4.2. DNA Mismatch Repair in Eukaryotes

The overall mechanism of DNA mismatch repair has been highly conserved in evolution and eukaryotes have a mismatch repair system like the *E. coli* MutHLS system. In general, repair in eukaryotes involves heterodimeric protein complexes, rather than the single proteins or homodimers employed by bacteria (Lindahl *et al.*, 1997). The initial steps of correction can be classed as primary and secondary recognition events (Lindahl *et al.*, 1997). Primary recognition and binding of mismatched DNA is carried out by homologues of the *E. coli* MutS protein, MSH2, MSH6 (GTBP) and MSH3, which can associate to form two different heterodimers

(Figure 1.3). The MutSα heterodimer [MSH2•MSH6] recognizes single base mispairs, single base loops and two base loops in repeated dinucleotide sequences. The MutSβ heterodimer [MSH2•MSH3] preferentially binds two, three and four base loops.

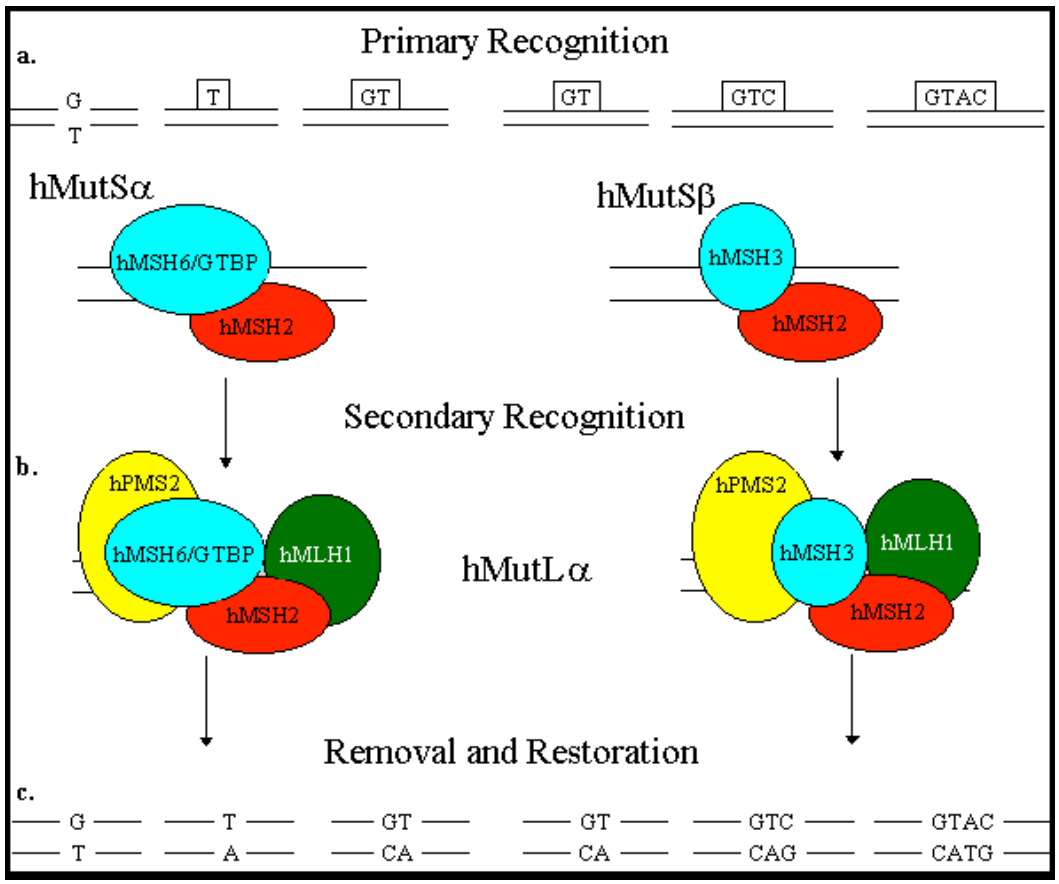

Figure 1.3. Model for eukaryotic mismatch recognition. a. Primary recognition: MutSα heterodimer preferentially recognizes single base mispairs, single base loops, and two base loops in repeated dinucleotide sequences, while MutSβ heterodimer preferentially binds two, three and four base loops. **b.** Secondary recognition: MutLα heterodimer is recruited by MutSα-DNA and MutSβ-DNA complexes. (Lindahl *et al.*, 1997).

MutSα mismatch recognition is regulated by adenosine nucleotide binding that acts as a molecular switch (Gradia *et al.*, 1997; Gradia *et al.*, 1999). The MutSα complex is ON (binds mismatched nucleotides) in the ADP-bound form and OFF in

the ATP-bound form. This ADP →ATP exchange converts the MutSα complex into a "sliding clamp" that diffuses along the DNA. Stochastic loading of multiple MutSα sliding clamps onto mismatch-containing DNA leads to activation of the repair machinery (Gradia *et al.*, 1999).

The secondary recognition event involves the MutLα heterodimer, which is composed of two homologues of the *E. coli* MutL protein, MLH1•PMS2. The MutLα heterodimer binds both the MutSα-DNA and MutSβ-DNA complexes (Figure 1.3). Cells with inactivating mutations in either of these components are completely mismatch repair-deficient. Following mismatch recognition, the DNA strand with the incorrect base is excised and new DNA synthesized by DNA polymerase using the nonmutated strand as a template. Finally, DNA ligase seals the gaps and completes repair.

Eukaryotic DNA is not methylated at GATC sites and no eukaryotic MutH homologue has been identified, so some other method of strand discrimination must exist. One hypothesis is that gaps between the Okazaki fragments on the daughter strand may specify the strand for mismatch repair (Boland, 1998). The DNA replication protein, proliferating cell nuclear antigen (PCNA), has been shown to associate with MLH1 and MSH2 and participate in an early step of mismatch repair, possibly strand discrimination (Umar *et al.*, 1996). Recently, researchers cloned a human gene encoding a protein that complexes with MLH1, binds to methyl-CpG-containing DNA, and displays endonuclease activity (Bellacosa *et al.*, 1999). Deletion mutants lacking the methyl-CpG-binding domain exhibited microsatellite instability, suggesting that cytosine methylation may have a role in human DNA

MMR and that this protein could be a eukaryotic homologue of the MutH endonuclease.

1.3.5. Mouse Models for HNPCC

Loss of DNA MMR is a rate-limiting step in the etiology of tumors associated with HNPCC in humans (Lynch and Smyrk, 1996). Mutations in *MLH1* and *MSH2* account for the majority of HNPCC kindreds with germ line mutations (Bronner *et al.*, 1994; Fishel *et al.*, 1993; Leach *et al.*, 1993; Papadopoulos *et al.*, 1994; Nicolaides *et al.*, 1994). Studies using mouse models have been designed to define the role of individual MMR genes in cancer susceptibility. They aim to address, first, whether constitutional DNA MMR deficiency in mice results in high levels of DNA replication errors *in vivo* and, second, whether the high level of spontaneous mutation correlates with spontaneous tumor development (Reitmair *et al.*, 1996; Prolla *et al.*, 1998; de Wind *et al.*, 1998; Edelmann *et al.*, 1999).

In a study using *Msh2*-deficient mice (de Wind *et al.*, 1998), it was observed that all *Msh2*$^{-/-}$ mice died before 1 year of age. Most of those animals had succumbed to lymphoma (mostly of T cell origin) before 30 weeks (Reitmair *et al.*, 1996; de Wind *et al.*, 1998). *Msh2*-deficient mice exposed to the exogenous mutagen ethyl-nitroso-urea (ENU) succumbed to lymphoma much earlier (14 weeks) than wild-type control mice (27 weeks). The early onset and 100% incidence of tumorigenesis in *Msh2*-deficient mice corroborated the increased risk for MMR-deficient cells to undergo oncogenic transformation (de Wind *et al.*, 1998). *Mlh1*-deficient mice also showed high levels of microsatellite instability and developed

lymphomas, intestinal adenomas and sarcomas (Prolla *et al.*, 1998; Edelmann *et al.*, 1999), similar to *Msh2*-deficient mice.

Pms2- and *Pms1*-deficient mice display a different pattern of tumor development. *Pms2*$^{-/-}$ mice showed frequent alterations in both mononucleotide and dinucleotide repeats (Prolla *et al.*, 1998; Edelmann *et al.*, 1999) and succumbed to lymphoma and sarcoma, but did not develop adenomas or adenocarcinomas. On the other hand, mice deficient for the *Pms1* gene showed only a small effect on mutations in mononucleotide repeats, did not show any defects in dinucleotide repeats, and did not develop tumors (Prolla *et al.*, 1998).

1.3.6. Mechanism of Tumorigenesis in HNPCC

Defects of MMR genes in tumors from HNPCC patients lead to a genetic instability in which short repeated sequences (microsatellites) are characteristically altered (Aaltonen *et al.*, 1993; Thibodeau *et al.*, 1993; Peltomaki *et al.*, 1993b; Lindblom *et al.*, 1993). This instability is indicative of a high mutation rate, which is believed to result in a rapid accumulation of somatic mutations in genes that direct pathways involved in tumor progression. Mutations in critical genes are accelerated and HNPCC patients develop carcinomas at an average age of 42, more than 20 years earlier than the general population (Lynch *et al.*, 1993).

Remarkably, the tissue distribution of tumorigenesis in HNPCC patients is limited to the colon, even though DNA MMR genes have a ubiquitous role in limiting mutations. This tissue specificity may be related to the fact that MLH1 and MSH2 proteins are highly expressed in the epithelium of the digestive tract (Fink *et*

al., 1997). Defective DNA MMR in such a highly proliferative tissue could lead to more rapid accumulation of mutations in those genes with mono- or di-nucleotide repeats (de Wind *et al.*, 1998). Such frameshift mutations, associated with alterations in normal mismatch repair, have been reported in several downstream genes, including *TGFβRII* (Markowitz *et al.*, 1995), *IGFIIR* (Souza *et al.*, 1996), *BAX* (Rampino *et al.*, 1997) and *MSH3* and *MSH6* (Yamamoto *et al.*, 1998).

1.4. Neurofibromatosis Type 1

Neurofibromatosis type 1 (NF1), also known as von-Recklinghausen's disease or peripheral neurofibromatosis, is a common autosomal dominant disorder. The hallmark of NF1 is the presence of multiple benign cutaneous neurofibromas consisting of a mixture of Schwann cells, fibroblasts, and mast cells (Lott and Richardson, 1981). Other clinical features include café au lait spots, freckling of the axilla and groin, and pigmented nodules of melanocytic origin in the iris, known as Lisch nodules. While these are the most commonly noted signs in NF1, the disease is characterized by a variable number of diverse pathologies throughout the body, including cutaneous, osseous, hematological, developmental, and nervous system abnormalities (Riccardi, 1992). Despite recent advances in the understanding of the molecular basis of NF1, these clinical criteria continue to be the most reliable means for making the diagnosis (Grifa *et al.*, 1995). The two major life-threatening complications of NF1 are hypertension and a significantly higher rate of malignancy (Zoller *et al.*, 1995; Sorensen *et al.*, 1986).

1.4.1. Incidence of Neurofibromatosis Type 1

Several studies were carried out in an attempt to ascertain the frequency of NF1. Littler and Morton (1990) reviewed data from four studies and found a carrier incidence for NF1 at birth of 1 in 2500. The gene frequency was estimated to be 0.0002. New mutations were found to be responsible for approximately 56% of cases. Lazaro *et al.* (1994) gave the incidence of NF1 as approximately 1 in 3,500 and estimated that about half of NF1 cases are due to new mutations. Garty *et al.* (1994) found an unusually high frequency of NF1 in young Israeli adults. They surveyed 374,440 17-year-old Jewish recruits for military service and found 390 with signs and symptoms of NF1 -- an incidence 2 to 5 times greater than previously reported. In this group, NF1 was more common in recruits whose parents were of North African and Asian origin (1.81 per 1,000 and 0.95 per 1,000, respectively) and less common in those of European and North American origin (0.64 per 1,000). All of these differences were statistically significant. The epidemiologists suggested that the increased incidence of NF1 in this group might be due to advanced age of the recruits' parents and/or a founder effect.

1.4.2. *NF1* Gene Structure

The *NF1* gene was isolated by positional cloning (Wallace *et al.*, 1990; Cawthon *et al.*, 1990; Viskochil *et al.*, 1990) and maps to chromosome region 17q11.2 (van Tuinen *et al.*, 1987). It consists of at least 59 exons spanning over 350 kb of genomic DNA (Wallace *et al.*, 1990; Li *et al.*, 1995; Goldberg and Collins, 1991). In the central region of neurofibromin (*NF1* gene product) there is a 360 amino acid region, encompassing exons 21-27a, that shows high homology (Figure

1.4) to the catalytic domain of the mammalian GTPase activating protein (GAP) (Xu *et al.*, 1990; Ballester *et al.*, 1990). This region of the *NF1* gene product is called the NF1 GAP-related domain (GRD) (Xu *et al.*, 1990; Ballester *et al.*, 1990).

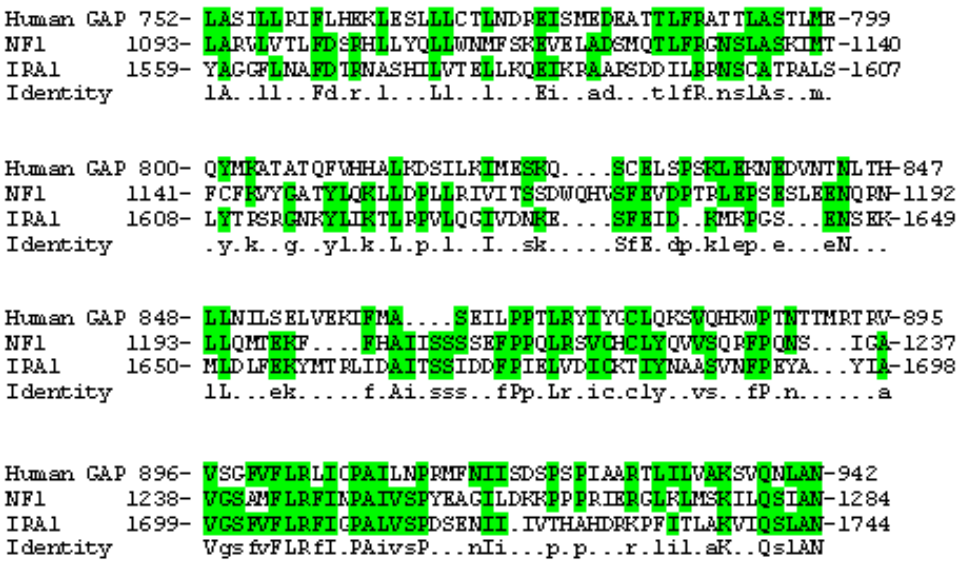

Figure 1.4. Sequence alignment of *GAP*, *NF1* and *IRA1* gene products. Shown is the region (190 residues) with highest homology between the human GAPa, NF1, and yeast IRA1 proteins. Gaps were introduced to allow the best alignment. Aligned identical residues are shaded. Consensus sequence summarizes conserved residues: upper case letters indicate residues identical in all three proteins, and lower case residues indicate residues shared in any two of the three proteins (Xu *et al.*, 1990).

Three genes, *EVI2A*, *EVI2B*, and *OMGP*, transcribed in the opposite orientation to *NF1*, are embedded within intron 27 (Cawthon *et al.*, 1991). A K3 pseudogene, transcribed in the same orientation to *NF1*, lies in intron 37 (Xu *et al.*, 1992).

1.4.3. *NF1* Gene Expression

NF1 is transcribed as an mRNA of 11-13 kb. This transcript encodes a protein (neurofibromin) of 2818 amino acids with an estimated molecular weight of 327 kDa (Wallace *et al.*, 1990). *NF1* is widely expressed in a variety of human and mammalian tissues (Danglot *et al.*, 1995; Marchuk *et al.*, 1991; Suzuki *et al.*, 1991; Takahashi *et al.*, 1994). *NF1* gene expression is regulated by three different mechanisms, including alternative splicing of the mRNA transcript, mRNA editing, and unequal allelic expression (reviewed in Skuse and Cappione, 1997). Aberrations *NF1* RNA processing might regulate intracellular neurofibromin levels and, thus, explain the great variation in expressivity of disease traits.

1.4.3.1. Alternative Splicing

The multiple *NF1* transcripts are summarized in Table 1.1 (Skuse and Cappione, 1997). The different *NF1* isoforms can be placed into two main groups: first, the transcripts differing in GRD (type I, type II, and type 4) and second, the transcripts differing in other coding regions. The two best-characterized transcripts differ by the inclusion or exclusion of exon 23a within the *NF1* GRD. The type I transcript excludes exon 23a, while the type II transcript includes exon 23a (63 bp) and introduces 21 amino acids into the resulting neurofibromin. Both transcripts are expressed in normal tissues; however, in brain tumors, there is an increased expression of the type II transcript (Suzuki *et al.*, 1991; Platten et al., 1996).

Table 1.1. Expression of Alternative Transcripts

Transcript	Alternative Exon(s)	Neurofibromin	Tissue Expression	GAP Activity
9br	9br	+ 10 residues	CNS, brain tumors (↓)	Normal
Type II	23a	+ 21 residues	all tissues, brain tumors (↑)	Reduced
Type 3	48a	+ 18 residues	cardiac, skeletal muscle	Present
Type 4	23a, 48a	+ 21, +18 residues	cardiac, skeletal muscle	Present
N-Isoform[1]	Δ11 to 49	Δ548 to 2815	brain tissue, brain tumors	Absent

[1]N-Isoform excludes exons 11-most of 49

Another transcript that includes exon 9br is transcribed only in the central nervous system. In brain tumors, its expression is reduced (Danglot *et al.*, 1995). Platten and coworkers reported the absence of the 9br transcript in optic nerve astrocytomas as well (Platten *et al.*, 1996).

The type 3 transcript includes exon 48a and is expressed in cardiac and skeletal muscles (Gutmann *et al.*, 1993). The type 4 transcript includes both exon 23a and exon 48a (Gutmann *et al.*, 1995) and is also expressed in skeletal and cardiac muscles. The N-isoform excludes exon 11 and most of exon 49; it is expressed both in normal brain and in brain tumors (Takahashi *et al.*, 1994).

1.4.3.2. mRNA Editing

In addition to the expression of alternative transcripts, the *NF1* mRNA is a subject to another mechanism of RNA processing, namely mRNA editing. Editing is a form of post-transcriptional modifications by which the sequence of the mRNA is changed from that prescribed by the encoding DNA. These changes in the mRNA sequence may involve either base modifications or base substitutions (Smith and Sowden, 1996; Ashkenas, 1997).

Base modification mRNA editing involves chemical modification of existing nucleotides to convert them into different ones. For example, the cytidine at position 3916 in the *NF1* mRNA transcript maybe deaminated to uracil (Skuse *et al.*, 1996). This modification introduces an in-frame stop codon into the 5' portion of the NF1 GRD, which is expected to result in a truncated neurofibromin completely lacking GTPase activating function. Thus, mRNA editing can result in loss of tumor suppressor activity without the involvement of mutations in the *NF1* gene itself.

Base substitution mRNA editing involves the addition, deletion, or replacement of specific nucleotides within the target transcript. Site-specific editing of the *NF1* transcript was identified by sequence homology of a mooring sequence in *NF1* to the motif responsible for editing in the apolipoprotein B mRNA (Skuse *et al.*, 1996). The editing site required for the chemical modification of a cytosine to uracil consists of three motifs: regulator, spacer, and mooring sequence. The mooring sequence was shown to be the critical element for site-specific editing (Backus and Smith, 1991; Skuse *et al.*, 1996). The editing process involves the assembly of an "editosome" composed of two RNA binding proteins and a cytidine deaminase at the

editing site. The assembled editosome chemically converts cytidine to uracil via deamination.

Cappione and coworkers (1997) investigated whether elevated levels of *NF1* mRNA editing could inactivate the *NF1* tumor-suppressor function by comparing the levels of edited *NF1* mRNA in tumor and nontumor tissue samples removed from the same NF1 patients. Tumor tissue contained higher levels of edited *NF1* mRNA than normal tissue from the same individual. Comparison of nontumor tissue from NF1 individuals with tissue from normal individuals revealed no significant difference in the level of *NF1* editing. These results suggest that low levels of *NF1* mRNA editing may appropriately regulate *NF1* gene expression but that high levels of mRNA editing may contribute to the development of benign neurofibromas and possible progression toward malignant tumors (Cappione *et al.*, 1997). Thus, mRNA editing provides another level by which gene expression can be regulated and the resulting protein diversity can be expanded.

1.4.4. *NF1* Gene Product: Neurofibromin

Using antibodies raised against both fusion proteins and synthetic peptides, a specific protein of about 250 kDa was identified by both immunoprecipitation and immunoblotting (Gutmann *et al.*, 1991). The protein was detected in human, rat, and mice tissues and appears to be expressed in all tissues. Based on the observed homology between the *NF1* gene product and members of the GTPase-activating protein (GAP) superfamily, the name NF1-GAP-related protein (NF1-GRP) was suggested.

DeClue and coworkers (1991) immunized rabbits with a bacterially synthesized peptide corresponding to the GAP-related domain of NF1 (NF1-GRD). In HeLa cell lysates, these antisera detected a 280-kDa protein, corresponding to the *NF1* gene product. Neurofibromin was present in a large molecular mass complex in fibroblast and Schwannoma cell lines and appeared to associate with a very large protein (400-500 kDa) in both cell lines.

1.4.4.1. Neurofibromin Structure

Neurofibromin, a 250 kDa hydrophilic protein, consists of 2818 amino acids (Xu *et al.*, 1990). Several studied have shown that neurofibromin is structurally related to the Ira (inhibitors of Ras activators) proteins of yeast and to the GAP protein of mammalian cells (Xu *et al.*, 1990; Buchberg *et al.*, 1990). Other studies showed the functional relationships between these proteins (Ballester *et al.*, 1990). The high homology between neurofibromin and GAP is limited to the catalytic domain; however, the homology between neurofibromin and Ira1/ Ira2 extends beyond the catalytic domain, suggesting that these structurally conserved regions have conserved biological functions as well (Ballester *et al.*, 1990).

The neurofibromin domain encoded by exons 21-27b shows strong homology to the GTPase-activating proteins (GAP) superfamily (Scheffzek *et al.*, 1998). This domain is referred to as the functional GAP-related domain (NF1-GRD) and thus far, represents the only defined segment of neurofibromin. X-ray crystallography of the NF1-GRD catalytic fragment comprising residues 1198-1530 (NF1-333) revealed

NF1-GRD as a helical protein (Figure 1.5) that structurally resembles the corresponding fragment derived from p120GAP (GAP-334) (Scheffzek *et al.*, 1998).

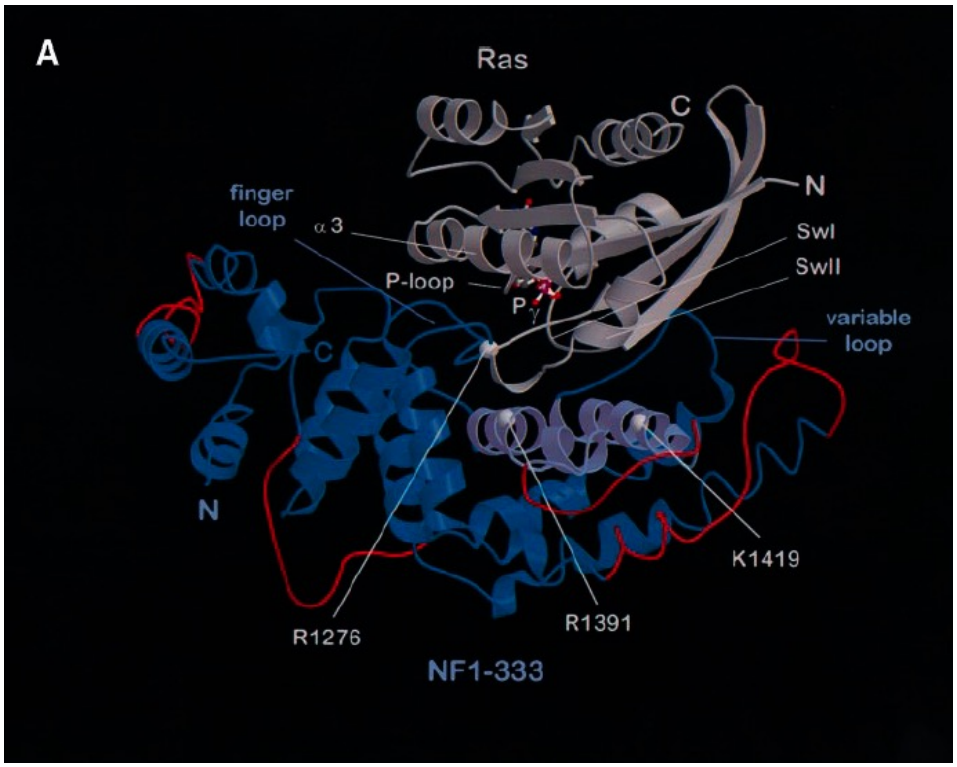

Figure 1.5. NF1-GRD interaction with Ras. Hypothetical complex between Ras (above) and NF1-333 (below) modeled according to the crystal structure of the Ras-GAP complex. Point mutations that affect the interaction with Ras are indicated by small spheres. (Scheffzek *et al.*, 1998)

This helical domain consists of two domains: a central domain ($NF1_c$) comprised of segments 1253-1304, 1331-1403 and 1412-1463, and an external domain ($NF1_{ex}$) comprised of segments 1206-1252, 1485-1503 and 1514-1530. A groove on the surface of $NF1_c$ has been identified as the Ras-binding groove based on structural comparisons of GAP-334 and NF1-333. This central domain represents the minimum catalytic domain of the Ras-GAP modules (Scheffzek *et al.*, 1998).

1.4.4.2. Neurofibromin Functions

Neurofibromin appears to act as a tumor suppressor since loss of heterozygosity at the *NF1* locus has been observed in DNA isolated from NF1 patients (Sawada *et al.*, 1996). The identification of a domain with structural homology to the mammalian GTPase activating protein p120GAP (Ballester *et al.*, 1990) has helped in understanding the function of the *NF1* gene product.

1.4.4.2.1. Tumor Suppressor

NF1 patients have multiple benign tumors, which are predisposed to malignant transformation. The presence of a domain in neurofibromin with high homology to the catalytic domain of mammalian GAP and yeast Ira1/Ira2 proteins, which can downregulate $p21^{ras}$ activity, suggested that *NF1* might function as a tumor suppressor gene. Loss of heterozygosity observed in *NF1* appears to confirm neurofibromin's role as a tumor suppressor (Sawada *et al.*, 1996).

Over 80% of germline mutations appear to result in severe truncation of neurofibromin (reviewed in Shen *et al.*, 1996). Skuse and Cappione (1997) reviewed the possible molecular basis for the wide clinical variability observed in NF1, even among affected members of the same family (Huson *et al.*, 1989) and suggested that alternative splicing and mRNA editing may be involved. They proposed that the classical 2-hit model for tumor suppressor inactivation (Knudson, 1993) be expanded to include post-transcriptional mechanisms that regulate *NF1* gene expression, reasoning that aberrations in these mechanisms may play a role in the observed clinical variability (Skuse and Cappione, 1997).

1.4.4.2.2. GTPase Activating Protein (GAP)

The GAP-related domain (GRD) encoded by exons 20-27b is the only region of neurofibromin to which a biologic function has been ascribed. Biochemical analysis has shown that the GAP-related domain of neurofibromin can accelerate the conversion of the active GTP-bound Ras to inactive GDP-bound Ras and thus, downregulate Ras activity (Shen *et al.*, 1996).

Ras acts as a molecular switch (Figure 1.6): switched ON when bound to GTP and switched OFF when bound to GDP. This switch involves conformational changes in Ras that are controlled by two classes of enzymes, the guanine nucleotide exchange factors (GEF) and the GTPase activating proteins (GAP). GEF proteins bind Ras and promote the dissociation of GDP, thus, allowing Ras to bind GTP and switch on. GAP proteins, such as neurofibromin, accelerate the slow intrinsic GTPase activity of Ras-GTP, switching Ras off.

In its active form, Ras triggers a kinase signal cascade first binding Raf, a serine threonine kinase, which phosphorylates and activates MEK, a tyrosine /serine protein kinase, that phosphorylates and activates MAP kinase. This MAP kinase phosphorylates many different proteins, including transcription factors, and regulates expression of cell cycle and differentiation proteins.

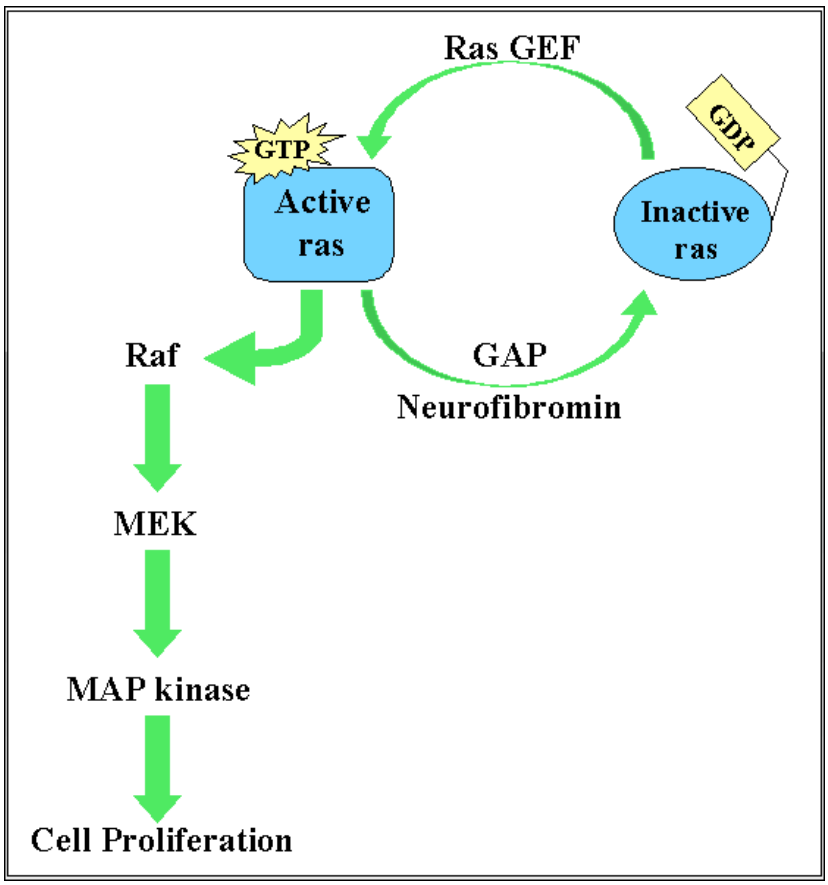

Figure 1.6. Regulation of Ras-induced cell proliferation by neurofibromin. Neurofibromin downregulates Ras activity by catalyzing the conversion of active Ras•GTP to inactive Ras•GDP. In this model, loss of neurofibromin would result in high levels of activated Ras•GTP, increased cell proliferation and tumor formation.

Two models involving neurofibromin and Ras have been proposed to explain the various clinical symptoms of NF1 (McCormick, 1995). In the upstream regulatory model, loss of neurofibromin would result in decreased GAP activity, which would lead to high levels of activated Ras•GTP and associated increased cell proliferation and tumor formation. In the downstream model, neurofibromin acts as an effector of Ras•GTP in signaling pathways controlling cell proliferation or differentiation.

1.4.4.2.3. Other Functions

The GTPase-activating activity of both the NF1-GRD peptide and the full-length neurofibromin can be inhibited by tubulin binding (Bollag *et al.*, 1993). The neurofibromin - tubulin interaction was demonstrated by their copurification. Tubulin binding determinants were localized to an 80-residue segment immediately N-terminal to the GAP related domain of neurofibromin (Bollag *et al.*, 1993). These observations suggest that neurofibromin serve as a link between tubulin and the growth regulator, Ras (Bollag *et al.*, 1993).

The NF1-GRD structural domain comprises only 13 % of the neurofibromin protein. The vast majority of mutations identified in the *NF1* gene, to date, do not disrupt the NF1-GRD. Furthermore, an isoform of neurofibromin, which lacks the NF1-GRD domain, has been identified (Suzuki *et al.*, 1992). These observations suggest that neurofibromin may have additional biological functions that remain to be identified.

1.4.5. *NF1* Mutation Rate

Mammalian gene mutagenesis can be influenced by genomic position (Wolfe *et al.*, 1989). Mutations in human genes have been found to occur non-randomly with respect to the surrounding DNA sequence (reviewed in Shen *et al.*, 1996). *NF1* has a mutation rate about 100-fold higher than the average mutation rate per generation per locus (Shen *et al.*, 1996). The mutations observed so far in *NF1* are not randomly distributed with respect to the DNA sequence, suggesting that the sequence composition of *NF1* also influences the mutation formation (Shen *et al.*,

1996). The high *NF1* mutation rate might be explained by the following three observations. First, the *NF1* gene spans large region (> 350 kb) of genomic DNA (Li *et al.*, 1995), which increases the probability for a random hit. Second, the *NF1* coding sequence contains 107 CpG islands and 40 microsatellites, both of which are known mutation hotspots (Rodenhiser *et al.*, 1997). Third, some of the *NF1* exons show high homology to pseudogenes, which may contribute in *NF1* mutagenesis by gene conversions (Cummings *et al.*, 1993).

1.4.5.1. Location of Mutations in *NF1*

Mutations in *NF1* occur non-randomly, with respect to the DNA sequence, throughout the coding region (Shen *et al.*, 1996). CpG dinucleotides appear to be a target for point mutations in exons 10a, 29, 31, and 42 (Valero *et al.*, 1994; Purandare *et al.*, 1994; Heim *et al.*, 1995). Particular sequence patterns in the human genome, including direct repeats, palindromes, symmetrical elements, and runs of identical bases, have been associated with insertions and deletions (Shen *et al.*, 1996). Examination of the flanking nucleotide sequences of defined *NF1* deletions and insertions has provided similar examples for such local environmental effects (reviewed by Shen *et al.*, 1996).

1.4.5.2. Types of Mutations in *NF1*

To date, 171 mutations have been reported in the Human Genome Mutation Database (Krawczak and Cooper, 1997; Human Genome Mutation Database, http://www.uwcm.ac.uk/uwcm/mg/search/120231.html, July 1999). These mutations (Figure 1.7) include 48 missense or nonsense nucleotide substitutions, 23 nucleotide

substitutions that affect splicing, 46 small deletions, 23 small insertions, one small insertion/deletion, and 24 gross deletions /duplications /complex rearrangements. The vast majority of *NF1* mutations lead to severe truncation of neurofibromin. Some nonsense and frame shift mutations have been associated with low levels of mRNA (reviewed in Shen et al, 1996).

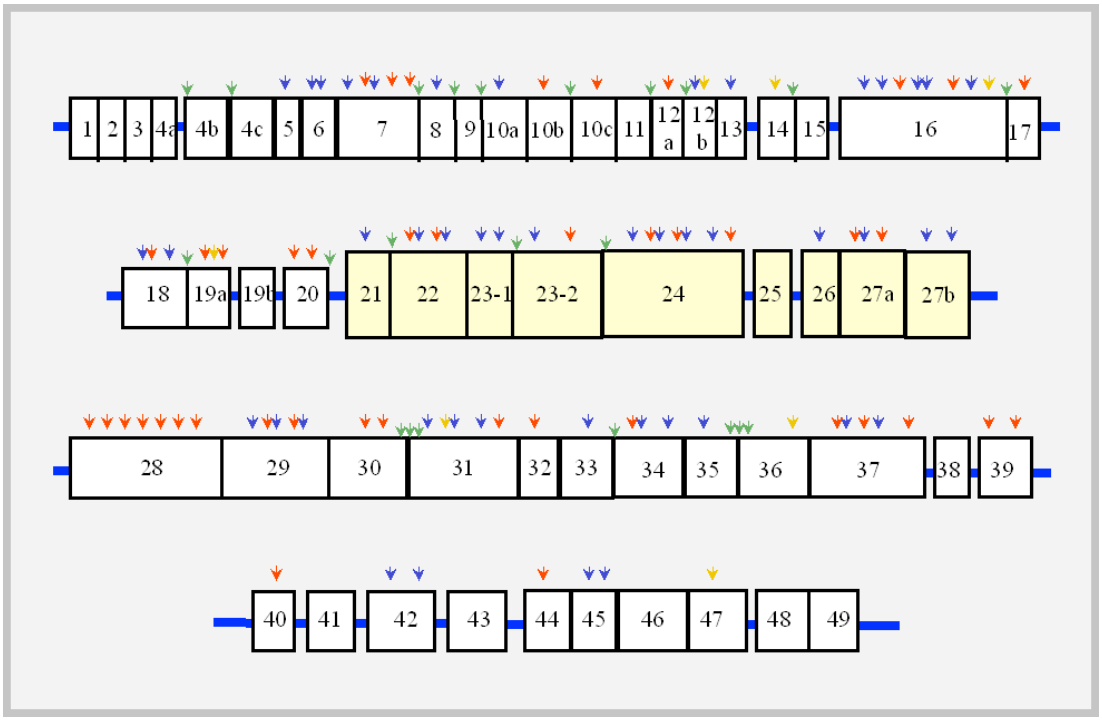

Figure 1.7. ***NF1* mutation map**. Mutations within the coding region of *NF1* are designated by arrowheads above each exon (not to scale). Mutation types: missense and nonsense nucleotide substitutions (blue); small deletions (red); small insertions (yellow); splice site nucleotide substitutions (green). NF1-GRD exons are depicted as yellow boxes.

1.5. Mutation Screening

Mutation screening and detection has become a valuable tool for the early diagnosis of cancer and for identifying the cause of the observed phenotype. Several screening protocols have been developed, including protein truncation test (PTT),

reverse transcriptase PCR (RT-PCR), heteroduplex analysis (HA), single-strand conformation polymorphism (SSCP), DNA sequence analysis, and restriction enzyme analysis. The optimal mutation detection technique would (1) be fast, (2) be able to screen large stretches of DNA with high sensitivity and specificity, (3) not involve expensive or elaborate instrumentation, (4) not require toxic or dangerous compounds and (5) provide information about the location and nature of the mutation. Unfortunately, no single procedure yet describe possesses all of these attributes.

1.5.1. Protein Truncation Test

The protein truncation test (PTT) rapidly detects frameshift and nonsense mutations that interrupt the reading frame (Roest *et al.*, 1993). Templates are generated by PCR, using cDNA synthesized by reverse transcription of mRNA (RT-PCR). A promoter is incorporated into forward primer. After *in vitro* transcription and translation assays are performed, the protein product is analyzed by gel electrophoresis. Truncating mutations are detected by comparing the molecular weight of the test protein to wild-type control protein.

1.5.2. RT-PCR

mRNA is isolated from blood and used as a template for RT-PCR, a PCR protocol utilizing an RNA template, exonic primers and reverse transcriptase (Guatelli *et al.*, 1990). The PCR products are then analyzed by gel electrophoresis. If a mutation is present, the PCR product may be smaller reflecting the smaller transcript. Alternatively, the PCR product may not be detected at all if there is no

mRNA transcript. This method is very useful for detecting exonic deletions that might not be detected using genomic DNA screening protocols (Hutter *et al.*, 1994).

1.5.3. Heteroduplex Analysis (HA)

Complementary single-stranded DNA derived from alleles that differ in sequence will include mismatched base pairs (heteroduplexes) if allowed to anneal. Heteroduplex molecules are formed by denaturing the normal and mutant DNA molecules at 95^{o}C and then allowing the single stands to anneal by cooling to room temperature slowly. Double-stranded heteroduplex molecules may show an altered electrophoretic migration in non-denaturing gels compared to homoduplexes of either allele (White *et al.*, 1992). The main advantage of HA is its simplicity, but its sensitivity is about 80-90% (Grompe, 1993).

1.5.4. Single Strand Conformation Polymorphism (SSCP)

Single strand conformation polymorphism or PCR-SSCP is one of the simplest methods for mutation detection. In this method, the target sequence of interest is amplified by PCR using labeled deoxynucleotide triphosphates. The PCR products are then denatured in formamide loading buffer by heating at 95°C for 2 minutes. The single-stranded molecules are then loaded on a non-denaturing polyacrylamide gel and size-fractionated at constant power using low voltage. The gel is then exposed to an X-ray film, which is developed after overnight exposure. DNA sequence variants often exhibit different electrophoretic mobility depending on the tertiary structures of the single-stranded DNA molecules (Hayashi and Yandell, 1993). Thus, mutant sequences usually appear as new bands in the autoradiograms.

If bands with altered mobility are detected, DNA sequence analysis is performed for confirmation.

Typically, a PCR-SSCP autoradiogram of one amplification product should give two bands (one for each of the separated strands) or a single band if the two strands are not resolved. Sometimes, however, more than two bands appear in the SSCP analysis of PCR products representing a single molecular species (a homozygous locus, for example). This is because the sequence may have more than one stable conformation. The appearance of bands of such iso-conformers is usually reproducible, both to position in the gel and relative abundance. Therefore, iso-conformer bands can be easily distinguished from bands of mutant alleles, since control samples analyzed in parallel in the same gel also have these bands (Hayashi, 1996).

The tertiary structure of a single-stranded DNA molecule changes under different physical conditions, like temperature and ionic environment, and accordingly, the sensitivity of SSCP depends on these conditions. However, the mutation detection sensitivity of PCR-SSCP is generally believed to be high -- up to 80% for fragments shorter than 300 bp (Hayashi and Yandell, 1993). Because the detection sensitivity is not 100%, the absence of a new band does not prove that there is no mutation in the analyzed molecule (Hayashi, 1996).

1.5.5. DNA Sequence Analysis

DNA sequence analysis is a fundamental technique in mutation detection. Double-stranded DNA templates can be used in standard dideoxy-sequencing by

denaturing the DNA prior to binding the oligonucleotide primer. Cycle-sequencing or linear amplification sequencing is a PCR sequencing approach, which increases the quality of sequences from double-stranded DNA templates. Like the standard PCR reaction, it uses the thermostable DNA polymerase and a temperature cycling format of denaturation, annealing, and DNA synthesis. The difference is that cycle-sequencing employs only one primer and includes a ddNTP chain terminator in the reaction. The use of only a single primer means that unlike the exponential increase in product during standard PCR reactions, the product accumulates linearly. Because of the high temperature at which the sequencing reactions are carried out and the multiple heat denaturation steps, small amounts of double-stranded PCR products may be sequenced reliably without a separate heat denaturation step.

The ABI PRISM™ 310 Genetic Analyzer (Perkin Elmer) powered by GeneScan™ software is a laser-induced fluorescence capillary electrophoresis system. As the labeled samples travel through the capillary and into the window, they are excited by the laser and emit light at a specific wavelength for each dye. The light is collected and separated by a spectrograph according to wavelength. It is collected onto a charge-coupled device (CCD) camera, so all four types of fluorescent emissions that are used to identify the A, G, C, and T extension reactions can be detected simultaneously. With ABI PRISM™ kits, fluorescent dye labels can be incorporated into DNA extension products using 3'-dye labeled dideoxy-nucleotide triphosphates (dye terminators). Thus the growing chain is simultaneously terminated and labeled with the dye that corresponds to that base. The fluorescent dye can be incorporated also by the use of 5'-dye labeled primers

(dye primers). Advantages of using the dye terminators over dye primers use of an unlabeled primer and performance of the four sequencing reactions simultaneously in one tube, thus, requiring fewer pipetting steps. On the other hand, dye primer labeling uses primers tagged with four different fluorescent dyes in four separate base-specific extension reactions. The products from these four reactions are then combined and loaded into a single gel lane. This is advantageous, since labeled primers are available for common priming sites.

1.5.6. Restriction Enzyme Analysis

A mutation may result in the introduction or elimination of a restriction enzyme recognition/cleavage site, which can be detected upon the incubation of test DNA sample with the corresponding restriction enzyme. The high specificity and sensitivity of restriction enzymes make this method a powerful tool for the screening of known mutations, and for the verification of newly detected mutations.

Restriction endonucleases recognize short DNA sequences and cleave double stranded DNA at specific sites within or adjacent to the recognition sequences. The recognition sequences are generally, but not always, 4 to 6 nucleotides in length and are usually characterized by palindromic sequences. In palindromic sequences the recognition site sequence is the same on each DNA strand when read 5'→3'. Some restriction enzymes cleave at the axis of symmetry yielding “blunt” ends. Others make staggered cleavages yielding “sticky” ends. Restriction enzyme cleavage is accomplished by incubating the enzyme with the DNA in appropriate reaction conditions. The amounts of enzyme and DNA, the buffer and ionic concentrations,

and the temperature and duration of reaction vary depending upon the specific application.

1.6. Hypothesis

Examination of the pedigree of the HNPCC kindred TF3 (Figure 1.1) reveals that the consanguineous marriage between two first cousins (III-5 and III-6 resulted in three offspring, who all died at an early age of leukemia and lymphoma. Both parents were afflicted with colorectal cancer and both were heterozygous for a C676T → Arg226Stop mutation in the DNA mismatch repair gene, *MLH1*. Analysis of clinical samples available for two of the children revealed that they were homozygous for the same *MLH1* mutation (Ricciardone *et al.*, 1999).

Interestingly, these two children were also afflicted with neurofibromatosis type 1 -- a phenotype not previously reported in HNPCC kindreds. We hypothesized that the homozygous truncating mutation in *MLH1* would have resulted in a complete lack of DNA mismatch repair activity and that, consequently, downstream mismatch mutations in the *NF1* gene would not be corrected and would result neurofibromatosis. Mutation analysis of the mononucleotide and dinucleotide repeat regions in the *NF1* coding region might reveal the molecular defect and clarify the genetic mechanism involved in this phenotype.

2. MATERIALS AND METHODS

2.1. Patient Samples

Patients in this study were referred to the Department of Molecular Biology and Genetics, Bilkent University (Ankara, Turkey) by collaborating physicians at Hacettepe University (Ankara, Turkey), Ankara University (Ankara, Turkey), and Çukurova University (Adana, Turkey). Informed consent was obtained from all participants in the study. The TF3 family pedigree is shown in Figure 1.1. The focus of this investigation, child IV-4, developed atypical chronic myeloid leukemia at 12 months and displayed clinical signs of neurofibromatosis (more than 10 abdominal café au lait spots and two fibromatous skin tumors). Two siblings, IV-3 and IV-2, also developed leukemia/lymphoma and died in early childhood. Clinical signs of neurofibromatosis were confirmed in one of the siblings (IV-3). The parents (III-5 and III-6) were both afflicted with colorectal cancer at an early age, 26 and 33 years old, respectively. Blood samples from the parents were collected in tubes containing EDTA. An archival DNA sample was available for child IV-4 and an archival bone marrow smear was available for the sibling (IV-3).

2.1.1. DNA Isolation

Genomic DNA was isolated from peripheral blood samples obtained from the child (IV-4), mother (III-5) and father (III-6). Genomic DNA was isolated from a bone marrow smear obtained from the sibling (IV-3). Genomic DNA was isolated by a method involving proteinase K lysis, phenol/chloroform extraction, and ethanol precipitation.

Blood was frozen in 700 µl aliquots in 1.5 ml eppendorf (Greiner Labortechnik, Frickenhausen, Germany) tubes at -80°C for at least one day before DNA isolation. Blood was thawed and diluted with 800 µl of 1× SSC (150 mM NaCl (Sigma, St. Louis, MO, USA), 15 mM sodium citrate, pH 7.0 (Sigma, St. Louis, MO, USA)), mixed by vortexing, and then centrifuged in a microfuge (Heraeus Instruments, Osterode, Germany) at 13,000 rpm for 1 minute. The supernatant was removed without disturbing the cell pellet and discarded into disinfectant. This step was repeated several times until a clean cell pellet was recovered.

Next, 800 µl extraction buffer (10 mM Tris HCl, pH 8.0) (Sigma, St. Louis, MO, USA), 10 mM Na_2EDTA (Sigma, St. Louis, MO, USA), 0.5% SDS (Merck, Frankfurt, Germany) and 10 µl proteinase K (20 mg/ml) (Appligene-Oncor, Illkirch, France) were added. The tube was vortexed briefly to resuspend the cell pellet. The suspension was incubated at 56°C for at least 1 hour. Incubation was done overnight if necessary to dissolve the cell pellet.

The DNA was then mixed with 400 μl phenol /chloroform /isoamyl alcohol (25:24:1) (all obtained from Carlo Erba, Milan, Italy) and vortexed for 60 seconds. This step was carried out in a fume hood. The mixture was then centrifuged for 5 minutes in a microfuge at 13,000 rpm. The upper aqueous layer (700 μl) was removed and placed into new tube. If the interface was not clear or if the DNA was sticky after this step, the supernatant was not removed; instead, an additional extraction step was carried out with 350 μl phenol /chloroform /isoamyl alcohol. The recovered supernatant was separated into multiple tubes (350 μl per tube).

The DNA was precipitated from solution by adding 35 μl of 3M sodium acetate, pH 5.2 (Merck, Frankfurt, Germany) and 700 μl ice-cold absolute ethanol (EtOH) (Delta Kimya, Ankara, Turkey) to each tube, mixing by inversion and placing at -20°C for 30 minutes. The DNA was pelleted by centrifugation in a microfuge for 15 minutes at 13,000 rpm. The DNA pellet was washed with 70% EtOH and centrifuged for another 5 minute at 13,000 rpm. After removing the alcohol with a micropipette, the tubes were left open on the bench top for approximately 30 minutes to allow ethanol to evaporate. Finally, the DNA was solubilized in 200 μl TE (10 mM Tris HCl [pH 8.0], 1 mM Na_2EDTA) by incubating at 56°C for at least 1 hour. DNA was then stored at -20°C.

For the sibling (IV-3), DNA was isolated from an archival bone morrow smear. The slide was first rinsed with 70% EtOH. Then cells were scraped from the slide into an eppendorf tube using a sterile blade. DNA extraction was initiated by adding 800 μl of extraction buffer (10 mM Tris HCl [pH 8.0], 10 mM Na_2EDTA,

0.5% SDS) and 10 μl proteinase K (20 mg/ml). The procedure was then continued as described above.

The integrity of the isolated DNA was checked by gel electrophoresis in 1.0% agarose (Sigma, St. Louis, MO, USA) and 1× TBE (90 mM Tris base (Sigma, St. Louis, MO, USA), 90 mM Boric acid (Sigma, St. Louis, MO, USA), 2 mM Na_2EDTA, pH 8.4). DNA samples were loaded into the sample wells and electrophoresed at 80 V for 1 hour. After the run, the gel was stained with ethidium bromide solution (0.03 mg/ml) (Sigma, St. Louis, MO, USA) for 15-30 minutes and rinsed with tap water. The DNA fragments were visualized using an UV transilluminator (Bio-Rad, Hercules, CA, USA).

2.1.2. Spectrophotometric Determination of DNA Concentration

The concentration and the purity of the isolated DNA were determined on the Beckman Spectrophotometer Du 640 (Beckman Instruments Inc., Fullerton, CA, USA) using the Beckman Instruments Du series 600 Spectrophotometer software program. Five μl of DNA were added to 995 μl TE, pH 8.0, and the absorbance values were measured at 260 nm and 280 nm. The A_{260} value allows calculation of the concentration of nucleic acid in the sample. An optical density value of one corresponds to approximately 50 μg/ml of double-stranded DNA. The A_{260}/A_{280} ratio provides an estimate of the purity of the nucleic acid. A pure preparation of DNA will have A_{260}/A_{280} ratio between 1.8 and 2.0. In the case of protein or phenol contamination, the ratio A_{260}/A_{280} will be significantly less than the values given above and accurate quantitation of the amount of nucleic acid will not be possible.

2.2. Polymerase Chain Reaction (PCR)

Exons within the GRD of *NF1* containing microsatellites were targeted for analysis. Polymerase chain reaction (PCR), a rapid procedure for *in vitro* enzymatic amplification of a specific segment of DNA (Mullis and Faloona, 1987), was performed to amplify the selected exons using genomic DNA as a template and intronic primers.

2.2.1. Primer Selection

We selected intronic primers previously published by more than one group in order to minimize the time needed for PCR optimization. Primer sequences are listed in Table 2.1. Primers for exons 16 and 23a were synthesized on the Beckman Oligo 1000M DNA synthesizer (Beckman Instruments Inc., Fullerton, CA, USA) at the Department of Molecular Biology and Genetics, Bilkent University (Ankara, Turkey). Primers for exons 21, 22, 23-2, and 27a were purchased from Iontek (Bursa, Turkey).

2.2.2. PCR Conditions

PCR kits were obtained from MBI Fermentas Inc. (Amherst, NY, USA). PCR reactions were performed in 0.2 ml Thermowell™ tubes (Corning Costar Corp., Cambridge, MA, USA) using the GeneAmp PCR system 9600 (Perkin Elmer, Foster City, CA, USA).

In general, 50-100 ng DNA was used as template. PCR was carried out in a reaction volume of 25 μl containing PCR buffer, 1.5-3.0 mM $MgCl_2$ (Table 2.1), 200

μM dNTP, 10 pmol forward primer, 10 pmol reverse primer and 1U *Taq* DNA polymerase. For radioactive PCR, the reaction volume was 25 μl and contained PCR buffer, 1.5-3.0 $MgCl_2$, 10 μM dNTP, 10 pmol forward primer, 10 pmol reverse primer, 1 U *Taq* DNA polymerase, and 1 μCi ^{32}P-dCTP (Amersham, Buckinghamshire, England).

Table 2.1. Intronic primer sequences used to amplify *NF1* exons

Exon (bp)	Primer Sequences	PCR Conditions	Ref.
16 (544)	5'TGGAT-AAAGCATAATTTGTCAAGT-3' 5'TAGAGAAAGGTGAAAAATAAGAG-3'	Annealing 55°C 3.0 mM $MgCl_2$	1, 2
21 (374)	5'AAATGAAAGTTTCATATAGAAATAC-3' 5'ATTTGCTATGTGCCAGGGAC-3'	Annealing 58°C 1.5 mM $MgCl_2$	1, 3
22 (331)	5'TGCTACTCTTTAGCTTCCTAC-3' 5'CCTTAAAAGAAGACAATCAGCC-3'	Annealing 55°C 1.5 mM $MgCl_2$	1, 3
23-2 (268)	5'CTTAATGTCTGTATAAGAGTCTC-3' 5'ACTTTAGATTAATAATGGTAATCTC-3'	Annealing 55°C 1.5 mM $MgCl_2$	1, 3
23a (446)	5'AGCCAGAAATAGTATACATGATTGGGT-3' 5'CTATTTTCTGCCAGAATTAGTAGA-3'	Annealing 55°C 3.0 mM $MgCl_2$	1, 3
27a (301)	5'CAGTTACAAGTTAAAGAAATGT-3' 5'CTAACAAGTGGCCTGGTGGCAAAC-3'	Annealing 58°C 1.5 mM $MgCl_2$	4

1. Li *et al.*, 1995; 2. Maynard *et al.*, 1997; 3. Upadhyaya *et al.*, 1997; 4. Abernathy *et al.*, 1997

There are three distinct events in PCR: template denaturation, primer annealing, and DNA synthesis. PCR parameters were an initial denaturation at 95°C for 2 minutes; 30 cycles of denaturation (95°C for 30 seconds), annealing (55°C for

30 seconds), and extension (72°C for 30 seconds); and a final extension at 72°C for 15 minutes.

PCR products were analyzed by loading 2 μl on a 2% agarose gel prepared in 1× TBE. Samples were run at 80 V for 1 hour. When the run was complete, the gel was stained in ethidium bromide solution (0.3 mg/ml) for 15-30 minutes and rinsed with tap water. The amplified fragments were visualized using an UV transilluminator.

2.3. Restriction Enzyme Cleavage of PCR Products

PCR products of exons 16 and 23a, 544 bp and 446 bp respectively, were cleaved by restriction enzyme digestion to get smaller fragments suitable for mutation detection by SSCP. Single restriction sites were found for *Eco*RII in exon 16 and for *Hin*fI in exon 23a. The enzymes recognition sites and resulting fragment lengths are listed in Table 2.2.

Table 2.2. Restriction enzymes used to cleave exons 16 and 23a

Exon (bp)	Enzyme	Recognition site	DNA Fragment Sizes
16 (544)	*Eco*RII	5' … CC↓(A/T)GG … 3'	307 bp + 237 bp
23a (446)	*Hin*fI	5' … G↓ANTC … 3'	311 bp + 135 bp

Restriction enzyme digestions with *Eco*RII and *Hin*fI (both obtained from MBI Fermentas Inc., Amherst, NY, USA) were performed in 20 μl reaction volumes of buffer supplied by the manufacturer (10 mM Tris-HCl [pH 8.5], 10 mM $MgCl_2$,

100 mM KCl, 0.1 mg/ml BSA). Reactions contained 2 μl of ^{32}P dCTP-labeled PCR product (~50 ng DNA) and 1U of enzyme. Reaction mixtures were incubated at 37°C for 2 hours.

The restriction digestion products were electrophoresed in a 2% agarose gel with 1× TBE at 80 V for 1 hour. After the run, the gel was stained with ethidium bromide solution (0.3 mg/ml) for 15-30 minutes and then rinsed with tap water. The DNA restriction fragments were visualized using an UV transilluminator.

2.4. Single Strand Conformation Polymorphism (SSCP)

Four different SSCP gel formulations were used that differed in the acrylamide: bisacrylamide ratio, acrylamide percentage, and the presence or absence of glycerol. Table 2.3 lists the components of the different acrylamide stock solutions. Table 2.4 lists the components of the different gel formulations.

Table 2.3. Acrylamide stock solutions used for SSCP gel preparation

	Acrylamide: Bisacrylamide [1]	
	50% (99:1)	**40% (75:1)**
Acrylamide [2]	49.5 g	39.5 g
Bisacrylamide [3]	0.5 g	0.53 g

[1] Total volume 100 ml; [2] Sigma, St. Louis, MO, USA; [3] Sigma, St. Louis, MO, USA

All the gel components except for APS and TEMED were combined and filtered using a Nalgene apparatus with 0.2 μm cellulose acetate filters (Corning Costar Corp., Cambridge, MA, USA). Vacuum was applied with a Hetomaster jet

water pump (Heto-Holten A/A, Allerød, Denmark) for at least 10 minutes in order to degas the acrylamide solution. Immediately before pouring, 10% APS and TEMED were added to the gel solution. The gel was allowed to polymerize for at least 2 hours.

Table 2.4. SSCP gel formulations used for mutation analysis

	Gel Formulation [1]			
	12.5% (99:1)	**10% (75:1)**	**6% (75:1)**	**5% (99:1)**
Acrylamide	25 ml	25 ml	15 ml	5 ml
ddH_2O	59 ml	59 ml	69 ml	85 ml
Buffer (10x)	6 ml TBE [2]	6 ml TBE	6 ml TBE	5 ml TPE [3]
Glycerol [4]	10 ml	10 ml	10 ml	---
10% APS [5]	400 µl	400 µl	400 µl	400 µl
TEMED [6]	40 µl	40 µl	40 µl	40 µl

[1] Total volume 100 ml;
[2] 0.9 M Tris base (Sigma, St. Louis, MO, USA), 0.88 M Boric acid (Sigma, St. Louis, MO, USA), 20 mM Na_2EDTA, pH 8.4) (Sigma, St. Louis, MO, USA);
[3] 0.6M Tris base, 0.4 M PIPES [1,4-piperazinediethanesulfonic acid] (Sigma, St. Louis, MO, USA), 20 mM Na_2EDTA [pH 6.8];
[4] Glycerol (Merck, Frankfurt, Germany);
[5] Ammonium persulfate (Sigma, St. Louis, MO, USA);
[6] N,N,N',N'-Tetramethylethylenediamine (Carlo Erba, Milan, Italy)

Six SSCP protocols listed in Table 2.5 were used in order to maximize mutation detection capability. Three gel electrophoresis apparatuses were used: EC 160 and EC 175 (both supplied by E-C Apparatus Corp., Holbrook, NY, USA) and Genomyx (Genomyx, Foster City, CA, USA). A Power-PAC 3000 power supply (Bio-Rad, Hercules, CA, USA) was used with the EC 160 and EC 175.

Table 2.5. SSCP protocols used for mutation detection

Protocol [1]	Apparatus	Gel Size	Acryl	A:B	Power	Buffer	Time
1	EC 160	33×42 cm	12.5 %	99:1	45 W	0.6× TBE	14 hr
2	EC 160	33×42 cm	10 %	75:1	45 W	0.6× TBE	12 hr
3	EC 160	33×42 cm	6 %	75:1	45 W	0.6× TBE	7 hr
4	EC 160	33×42 cm	5 %	99:1	40 W	0.5× TPE	3 hr
5	EC 175	15×28 cm	12.5 %	99:1	5 W	0.6× TBE	30 hr
6	Genomyx [2]	35×65 cm	10 %	75:1	20 W	0.6× TBE	9 hr

[1] Protocols 1-3, 5-6: Akyerli, MSc thesis, 1998; protocol 4: Kukita *et al.*, 1997

[2] Note: Genomyx protocol used 0.6× TBE for upper buffer and 1× TBE for lower buffer.

The SSCP reaction was performed by mixing 2 μl PCR product with 18 μl SSCP gel loading buffer (95% formamide (Sigma, St. Louis, MO, USA), 10 mM NaOH (Carlo Erba, Milan, Italy), 0.25% bromophenol blue (Sigma, St. Louis, MO, USA), and 0.25% xylene cyanol (Sigma, St. Louis, MO, USA)). The DNA solution was heated at 95°C for 2 minutes and kept on ice for at least 10 minutes before loading onto the gel. Electrophoresis was performed at constant power. Electrophoresis temperature was 4°C for protocols 1 through 5, the running temperature for protocol 6 was 25°C. After electrophoresis the gel was removed from the glass plates using Whatman 3MM paper (Whatman, Maidstone, England) and dried on the SGD 2000 slab gel dryer (Savant, Holbrook, NY, USA) at 80°C for 45 minutes. Radioactive bands were detected by autoradiography or phosphoimaging.

For autoradiography, the dried gel was placed into a cassette with X-ray film (Kodak, Rochester, NY, USA) and an intensifying screen. The cassette was placed

at −80°C for exposure. After exposure, the film was developed using a hyperprocessor developer (Amersham, Buckinghamshire, England).

Phosphoimaging was performed using the Molecular Imager® System, GS-525 (Bio-Rad, Hercules, CA, USA). The dried gel was placed into the cassette and a clean, erased screen was then placed over the gel. After exposure, the screen was scanned and the image was captured using Multi-Analyst software.

2.5. DNA Sequence Analysis

DNA sequence analysis of *NF1* exon 22 was performed using both the forward and reverse primers listed in Table 2.1. The PCR template was quantified by agarose gel electrophoresis using a ΦX174/*Hae*III DNA size marker (MBI Fermentas Inc., Amherst, NY, USA) of known concentration. Cycle sequencing reactions were set up in 0.2 ml Thermowell™ tubes (Corning Costar Corp., Cambridge, MA, USA). The 20 μl reaction volume contained 30-180 ng template PCR product, 3.2 pmol of primer (forward or reverse), and 4 μl terminator ready reaction mix (Thermo Sequenase™ dye terminator cycle sequencing kit, Amersham Life Science, OH, USA). The cycle sequencing reactions were performed in Perkin Elmer GeneAmp PCR 9600 system thermal cycler with the following parameters: 30 cycles of denaturation (96°C for 30 seconds), annealing (45°C for 15 seconds), and extension (60°C for 4 minutes).

Cycle sequencing products were precipitated by adding 7 μl 7.5 M ammonium acetate and 68 μl cold absolute ethanol and placing on ice for 15 minutes. The precipitated DNA was collected by centrifuging at 13,000 rpm for 15

minutes, washed with 250 μl cold 70% EtOH and air-dried. The DNA pellet was resuspended in 25 μl TSR (Template Suppression Reagent, PE Applied Biosystems, Foster City, CA, USA). The samples were heat-denatured at 95°C for 2 minutes and kept on ice for at least 5 minutes prior to loading for electrophoresis.

Electrophoresis was performed on the ABI PRISM™ 310 Genetic Analyzer (Perkin Elmer, Foster City, CA, USA). The DNA sample was injected onto a 47 cm × 50 μm capillary (PE Applied Biosystems, Foster City, CA, USA) containing POP6 (Performance Optimized Polymer 6, PE Applied Biosystems, Foster City, CA, USA) using a Hamilton 250 μl syringe. Genetic Analyzer Buffer with EDTA (PE Applied Biosystems, Foster City, CA, USA) was used as the running buffer. The module used for electrophoresis was Seq-POP6-Rapid-250 μl-A. The running conditions were injection time of 30 seconds at 2 kV, syringe pump time of 90 seconds, and collection time of 36 minutes at 50 kV. The heat plate temperature was set to 50°C.

The data was collected using ABI Data Collecting Software (version 1.0.4) during electrophoresis. After electrophoresis, the data were automatically analyzed by ABI Sequencing Analysis Software (version 3.0.1). The analyzed files were then imported into the Factura program to identify the unambiguous sequences. These analyzed sequences were then imported into the Sequence Navigator for alignment with the reference DNA sequence.

2.6. *Taq*I Restriction Enzyme Digestion

The wild-type *NF1* allele contains a *Taq*I site in exon 22 that is absent in the mutant allele. *Taq*I restriction enzyme digestion was performed in order to confirm

the C→T transition in *NF1* exon 22. The 20 μl reaction volume contained 2 μl PCR product in 1× incubation buffer V (Appligene-Oncor, Illkirch, France), and 1U of *Taq*I enzyme (Appligene-Oncor, Illkirch, France). Reaction mixtures were incubated at 65°C for 2 hours. The restriction digestion products were loaded into a 4% NuSieve 3:1 agarose (FMC Bioproducts, Rockland, ME, USA) prepared in 1× TBE. The gel was run for 3 hours at 50 V. After the run, the gel was stained with ethidium bromide solution (0.3 mg/ml) for 15-30 minutes and rinsed with tap water. The DNA fragments were visualized using a UV transilluminator.

2.7. Allele Specific Amplification of *MLH1*

MLH1 exon 8 reverse primers were designed for allele specificity at the 3' terminal nucleotide: 5'-GTTATCGACATACCA-3' for the mutant allele, and 5'-GTTATCGACATACCG-3' for the wild type allele. 5'-GCCATGAGACAATAA-3' was used as the forward primer (Ricciardone *et al.*, 1999).

The amplification reaction contained ~ 25 ng of genomic DNA and 10 pmol of each primer in a total volume of 25 μl of 1× PCR buffer, 1.5 mM $MgCl_2$, 200 μM dNTP, and 1U *Taq* DNA polymerase (MBI Fermentas Inc., Amherst, NY, USA). PCR parameters were an initial denaturation at 95°C for 2 minutes; 30 cycles of denaturation (94°C for 30 seconds), annealing (52°C for 60 seconds), and extension (72°C for 90 seconds); and a final extension at 72°C for 15 minutes. The PCR products were analyzed by loading 10 μl into 2% agarose gels prepared in 1× TBE. Samples were run at 80 V for 1 hour. When the run was complete, the gels were

stained in ethidium bromide solution (0.3 mg/ml) for 15-30 minutes and then rinsed with tap water. The amplified fragments were visualized using UV transilluminator.

3. RESULTS

3.1. Prioritization of *NF1* Exons for Mutation Detection

Mutation analysis was limited to those *NF1* exons containing microsatellites, because the probability of a mutation occurring in such sequences is higher than in other genomic sequences (Shen *et al.*, 1996). Analysis of the *NF1* coding region revealed 36 microsatellites in 26 exons, two microsatellites in the 5' untranslated region (UTR) and four microsatellites in the 3' UTR (Figure 3.1). Microsatellite sequences included mononucleotide, dinucleotide and trinucleotide repeat motifs (Table 3.1).

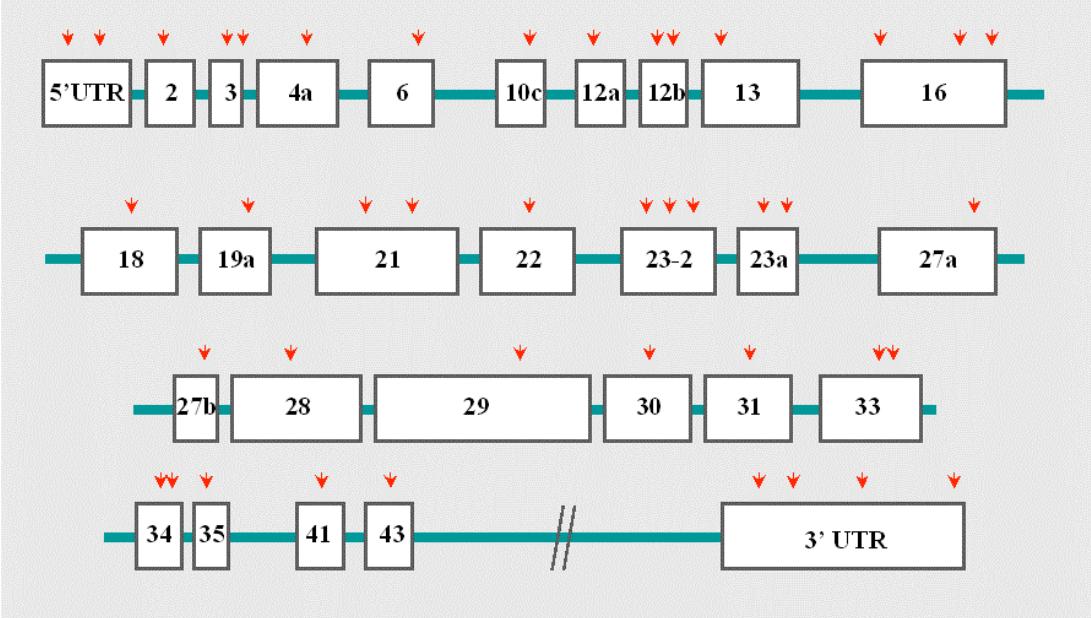

Figure 3.1. Microsatellites in *NF1* coding regions. Numbered rectangles represent *NF1* exons and lines represent introns. Arrows indicate the relative position of microsatellites.

Table 3.1. ***NF1*** **exons containing microsatellite repeats**

Exon	Position	Repeat	Exon	Position	Repeat
2	284	$(CA)_3$	23a	4348	$(A)_7$
3	424	$(A)_7$		4362	$(A)_6$
	437	$(TC)_4$	27a	4866	$(AC)_3$
4a	627	$(TC)_3$	27b	5011	$(T)_6$
6	1045	$(AT)_3$	28	5171	$(TC)_3$
10c	1804	$(CA)_3$	29	5720	$(AC)_3$
12a	1930	$(T)_6$	30	5827	$(TG)_3$
12b	2074	$(T)_6$	31	6085	$(ATG)_3$
	2165	$(CT)_3$	33	6560	$(CA)_3$
13	2224	$(C)_7$		6590	$(CT)_3$
16	2661	$(GGA)_3$	34	6757	$(TC)_3$
	2904	$(GT)_3$		6774	$(GA)_5$
	3027	$(T)_6$	35	6848	$(GA)_3$
18	3272	$(GA)_3$	41	7578	$(CTT)_3$
19a	3369	$(GAT)_3$	43	7893	$(C)_6$
21	3778	$(AC)_3$	5' UTR	42	$(C)_6$
	3813	$(GA)_3$		177	$(C)_6$
22	4015	$(CT)_3$	3' UTR	8733	$(T)_6$
23-2	4184	$(AG)_3$		8795	$(C)_6$
	4268	$(C)_6$		8913	$(T)_6$
	4285	$(GT)_3$		9018	$(AG)_3$

NF1 is a huge gene with a large number of exons. Therefore a prioritized sequence of analysis was designed in order to save time, effort, and money. We prioritized the *NF1* exons for mutation detection according to the criteria shown in

Table 3.2. Our highest priority was analysis of exons within the GRD, which if mutated, would alter the function of neurofibromin (Anglani *et al.*, 1993). Our second priority was analysis of an exon containing CpG islands previously described as mutation hot spots (Valero *et al.*, 1994; Rodenhiser *et al.*, 1997). Subsequent priorities were given to exons containing mononucleotide, dinucleotide and trinucleotide repeats, with priorities assigned based on structural tendency for DNA polymerase slippage (Trinh and Sinden, 1991). Exon 16, a priority 3 exon with a mononucleotide repeat, was included in the initial analysis since primers for this exon were already available in the department.

Table 3.2. *NF1* exon priorities for mutation detection

Criterion	Exons
GAP-Related Domain (GRD)	21, 22, 23-2, 23a, 27a
Multiple CpG islands	29
Mononucleotide repeat	3, 12a, 12b, 13, 16, 27b, 43
Dinucleotide repeat	2, 4a, 6, 10c, 18, 28, 30, 33, 34, 35
Trinucleotide repeat	19a, 31, 41

3.2. DNA Isolation

An archival DNA sample was obtained for the child (IV-4). Genomic DNA was isolated from peripheral blood samples obtained from the mother (III-5), father (III-6) and a wild-type control individual. DNA was also isolated from an archival bone marrow sample of the sibling (IV-3). All extracted DNAs were evaluated

quantitatively and qualitatively by UV spectrophotometry (Table 3.3) and/or agarose gel electrophoresis (Figure 3.2).

The A_{260}/A_{280} ratio gives information about the purity of the DNA. The A_{260}/A_{280} ratio of good quality DNA, not contaminated with proteins or phenol, usually ranges from 1.8 to 2.2. Although the values in Table 3.3 fall outside this range, this is most likely an artifact caused by low absorbance readings. Calculations are not very reliable when absorbance readings are below 0.100. A more concentrated DNA sample probably would have given more reliable absorbance readings. However, since the amount of DNA was limited, this was not done.

Table 3.3. Spectrophotometric analysis of genomic DNA samples

Sample	260 nm	280 nm	A_{260}/A_{280}	Dilution Factor	Concentration µg/ml
Mother	0.034	0.011	3.1	200	340
Father	0.036	0.012	3.0	200	360
Control	0.013	0.008	1.6	200	130

Agarose gel electrophoresis of the genomic DNA isolated from the mother, father and wild-type control revealed that the DNA was of high molecular weight and suitable for PCR, SSCP and DNA sequence analysis (Figure 3.2a). Agarose gel electrophoresis of the genomic DNA isolated from the sibling revealed that the DNA was degraded (Figure 3.2b). These results were not unexpected because the DNA had been isolated from an archival bone morrow smear that had not been preserved under perfect conditions. However, since the PCR product of *NF1* exon 22 is only

331 bp, this degraded DNA sample should still be sufficient for amplification of the target exon.

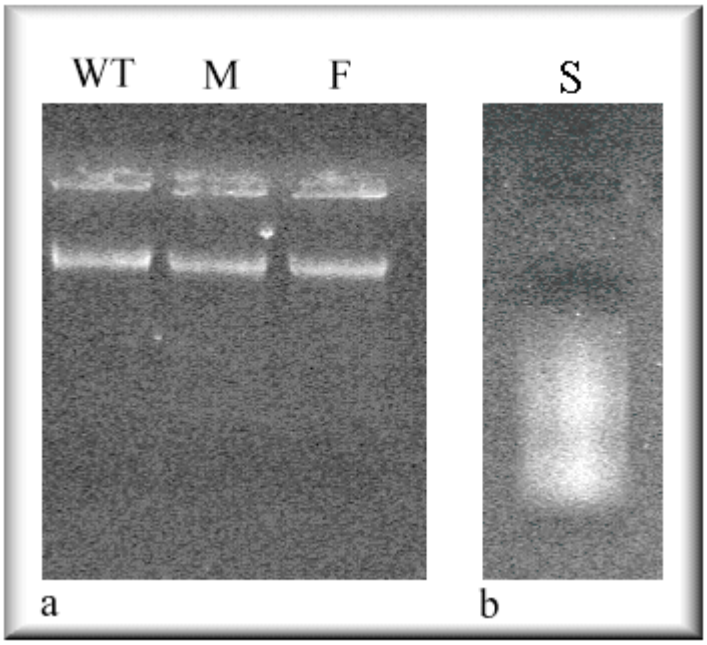

Figure 3.2. Agarose gel electrophoresis of extracted genomic DNA samples. Genomic DNA samples were electrophoresed in a 1% agarose gel with TBE at 80V for 1 hour. a. DNA isolated from wild-type control individual (WT), mother [III-5] (M), and father [III-6] (F). b. DNA isolated from sibling [IV-3] (S).

3.3. Polymerase Chain Reaction Optimization

PCR conditions, especially Mg^{++} concentration and annealing temperature, were optimized for specific amplification of the *NF1* exons. $MgCl_2$ concentrations between 1.5-3.0 mM and annealing temperatures between 55-60°C were tested. A positive control (*MLH1* exon 10) and a negative control (reaction mixture including *Taq* DNA polymerase without DNA) were included with every set of reactions. All PCR products were evaluated by 2% agarose gel electrophoresis. The optimal PCR parameters are listed in Table 3.4. PCR amplification using these conditions resulted

in production of a single DNA fragment -- no nonspecific amplification was observed (Figure 3.3). Comparison of the PCR product size with the ΦX174/*Hin*fI molecular marker revealed that all PCR products were of the expected size.

Table 3.4. PCR parameters for priority-one exons

Exon	PCR Product Size	Annealing Temperature	[Mg^{++}] mM
21	374 bp	58°C	1.5
22	331 bp	55°C	1.5
23-2	268 bp	55°C	1.5
23a	446 bp	55°C	3.0
27a	301 bp	58°C	1.5
16	544 bp	55°C	3.0

Note: Exon 16 is not a first priority exon, it was analyzed because primers were available in the department.

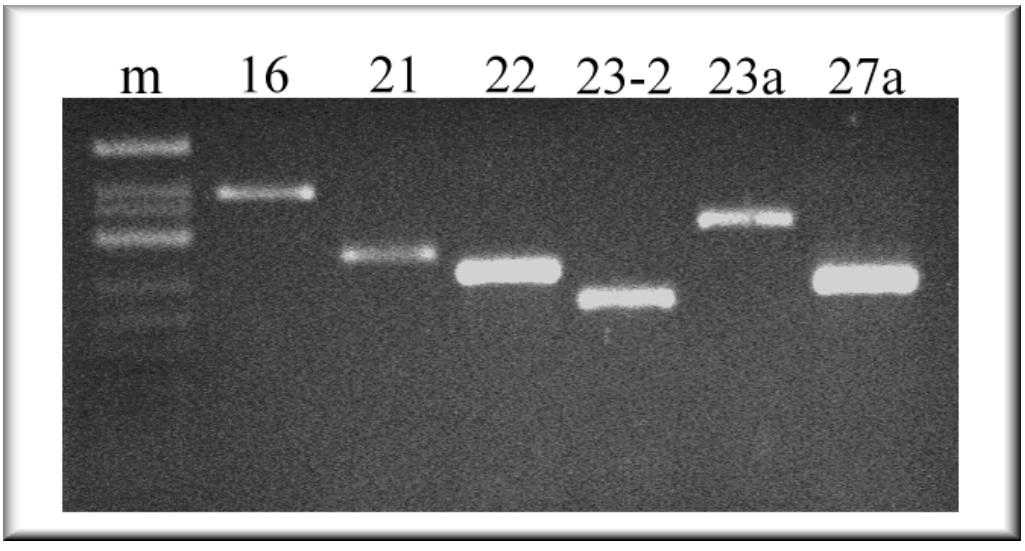

Figure 3.3. *NF1* exons amplified with optimized PCR protocols. PCR products were electrophoresed in 2% agarose gels with TBE at 80V for 1 hour. Lane labels represent *NF1* exons. Lane m contains the ΦX174/*Hin*fI molecular weight marker with 726, 553, 500, 427, 311, 249, and 200 bp fragments.

3.4. Restriction Digestion of *NF1* Exons 16 and 23a

The PCR products of *NF1* exon 16 (544 bp) and *NF1* exon 23a (446 bp) are too large for mutation detection by SSCP analysis, which is most sensitive for DNA fragments less than 300 bp (Hayashi and Yandell, 1993). These two exons were analyzed for appropriate restriction enzyme sites that could cleave the PCR products into smaller DNA fragments suitable for SSCP analysis. *Eco*RII was predicted to cleave exon 16 into two fragments (237 and 307 bp) and *Hin*fI was predicted to cleave exon 23a into two fragments (135 and 311 bp) as shown in Figure 3.4.

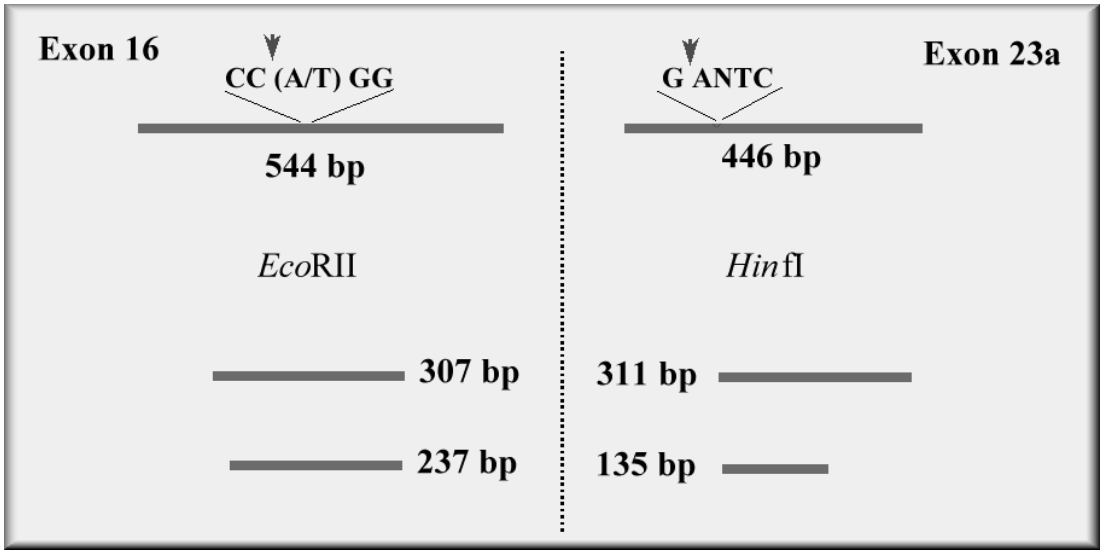

Figure 3.4. Restriction enzyme cleavage of *NF1* exon 16 by *Eco*RII and *NF1* exon 23a by *Hin*fI. In each panel, the upper band represents the PCR amplification product. Arrows designate restriction cleavage sites in the target sequences. Expected restriction DNA fragments are schematically shown at the bottom of the figure.

The *NF1* exon 16 and 23a DNA fragments obtained by PCR were subjected to restriction enzyme digestion with *Eco*RII and *Hin*fI, respectively. The digestion products were analyzed by agarose gel electrophoresis on 2% gels. Complete digestion of the PCR products into DNA fragments of the expected sizes was

observed, as shown in Figure 3.5. The lengths of these restriction enzyme-digested DNA fragments are suitable for mutation detection by SSCP analysis.

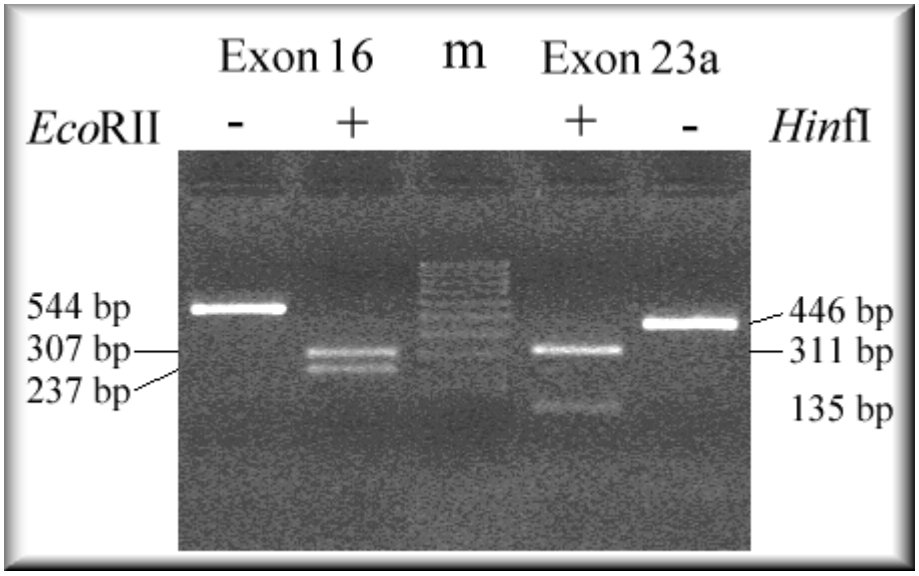

Figure 3.5. Analysis of EcoRII digestion of *NF1* exon 16 and *Hin*fI digestion of *NF1* exon 23a. DNA samples were electrophoresed in 2% agarose gels with TBE at 80V for 1 hour. Lanes with "-" sign designate samples that have not been treated with the restriction enzyme. Lanes with "+" sign designate samples treated with the restriction enzyme. Expected DNA fragment sizes are indicated in the margins.

3.5. Single Strand Conformation Polymorphism (SSCP) Analysis

NF1 mutation screening was carried out using SSCP protocols previously determined to have good detection capabilities. The six different SSCP protocols (Table 2.5) can be grouped into two main categories: first, conventional SSCP protocols (numbers 1, 2, 3, 5 and 6) that used TBE (Tris-Borate-EDTA, pH 8.4) plus glycerol as the buffering system (Akyerli, MSc Thesis, 1998); second, the low pH SSCP protocol (number 4) that used TPE (Tris-PIPES-EDTA, pH 6.8) without glycerol as the buffering system (Kukita *et al.*, 1997). For each *NF1* exon, PCR fragments were amplified by radioactive PCR using both the child's genomic DNA

as a template and control DNA, from the mother, father and a wild-type individual, as templates. The PCR products were then analyzed using the six different SSCP protocols and the mobility of the child's DNA fragment was compared to the mobility of the PCR fragments of the control individuals. A summary of the results is presented in Table 3.5. DNA isolated from CL 12826A, a cell line with a known mutation (1846-48 ΔAAG) in *MLH1* exon 16 was included as a positive control in all SSCP experiments performed.

Table 3.5. SSCP mobility shifts of DNA fragments

	SSCP Protocol					
	1	**2**	**3**	**4**	**5**	**6**
***NF1* exon 16**	-	-	-	-	-	-
***NF1* exon 21**	-	-	-	-	-	-
***NF1* exon 22**	-	+	+	+	-	-
***NF1* exon 23-2**	-	-	-	-	-	-
***NF1* exon 23a**	-	-	-	-	-	-
***NF1* exon 27a**	-	-	-	-	-	-
CL 12826	+	+	+	+	+	+

3.5.1. Conventional SSCP Protocols

DNA isolated from CL 12826 was included as a positive control in all SSCP experiments. This cell line has three base pair deletion in exon 16 of the *MLH1* gene that results in deletion of Lys codon 616. A representative SSCP analysis of this sample using protocol 5 (12.5% [99:1] acrylamide with EC 175 apparatus) is shown in Figure 3.6. The mutant allele migrates as two distinct single-stranded molecules,

while the wild-type allele migrates as a single broader band. This mutation was detected using all protocols (Table 3.5).

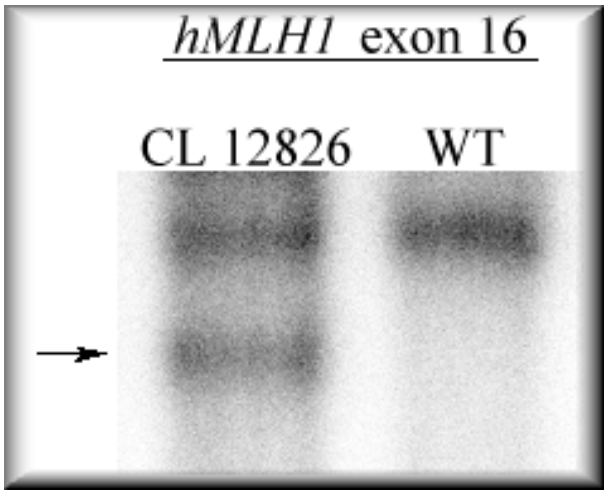

Figure 3.6. SSCP analysis of the positive control CL 12826 (*MLH1* exon 16, 1846-48 ΔAAG). Single-stranded DNA samples were electrophoresed in 12.5% [99:1] acrylamide on the EC 175 at 5 W constant power at 4˚C for 30 hours. Phosphorimager exposure was 10 hours. Arrow indicates band with altered mobility. Lanes: mutant cell line (CL 12826), wild-type control (WT).

Comparison of the SSCP results for *NF1* exons of the child with those of the mother, father and wild-type control individual revealed differential strand mobility for exon 22 that was detected using protocol 2 (10% [75:1] acrylamide) and protocol 3 (6% [75:1] acrylamide), both with the EC 160 apparatus) (Figure 3.7). As seen in the figure, although all four samples have two DNA bands, the upper band of the child's sample migrates more slowly than the upper bands of the control samples. This markedly different migration of the child's sample might reflect a mutation in the DNA sequence.

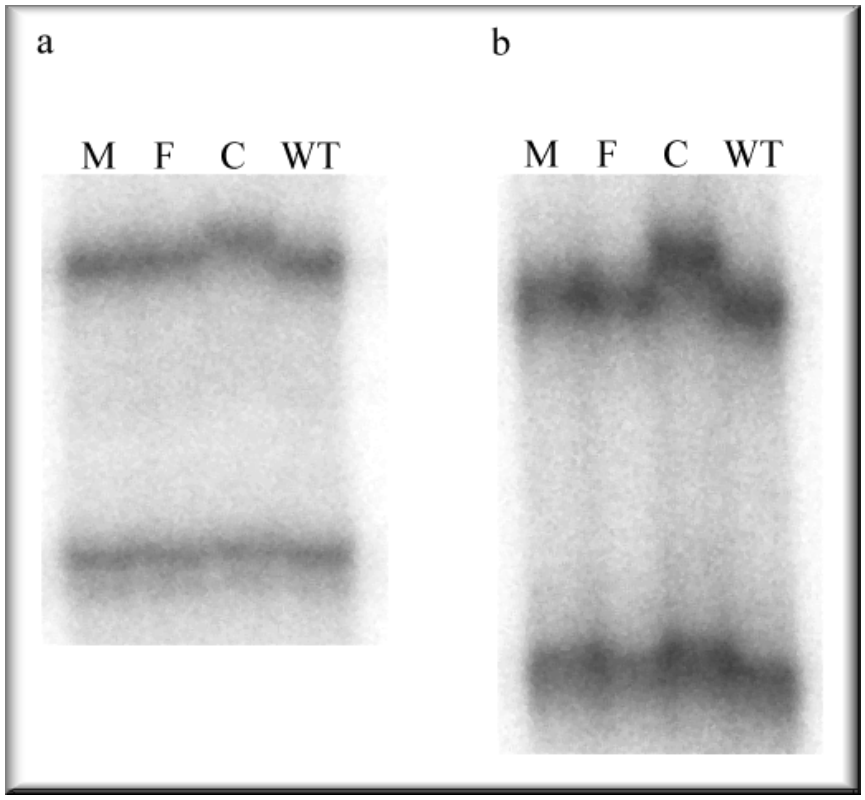

Figure 3.7. SSCP analysis of *NF1* exon 22. a. Electrophoresis of DNA samples in 10% [75:1] acrylamide on the EC 160 apparatus at 45 W constant power at 4°C for 12 hours. Phosphorimager exposure was 27 hours. **b.** Electrophoresis of DNA samples in 6% [75:1] acrylamide on the EC 160 apparatus at 45 W constant power at 4°C for 8 hours. Phosphorimager exposure was 36 hours. Lanes: mother (M), father (F), child (C), and wild-type control (WT).

NF1 exons 16, 21, 23-2, 23a, and 27a did not show any mobility shift in any of the 18 SSCP analyses performed. Figure 3.8 represents such a negative result, which was obtained for exons 23-2 and 27a using protocol 3 (6% [75:1] acrylamide with the EC 160 apparatus). In this figure, the child's DNA fragments appear to migrate the same as the control DNA fragments migrate suggesting that there are no sequence differences in these exons.

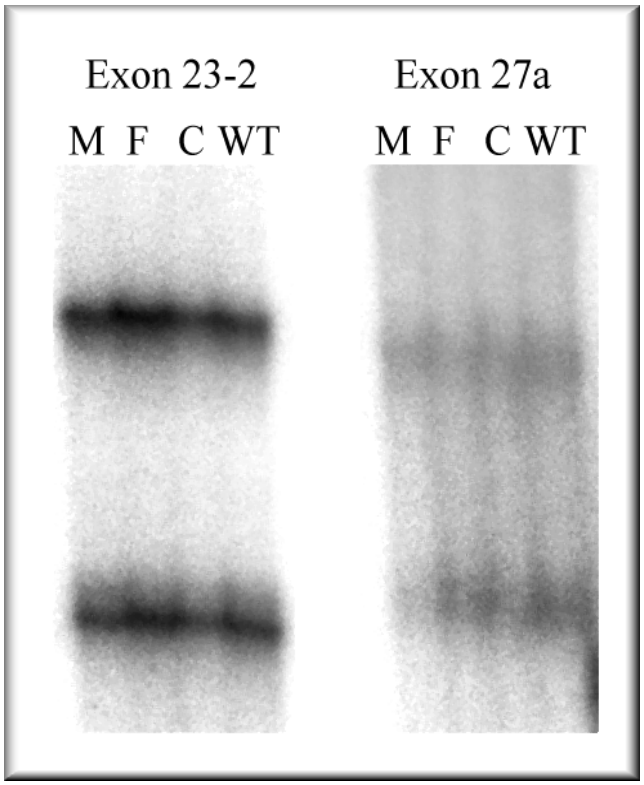

Figure 3.8. SSCP analysis of *NF1* exon 23-2 and *NF1* exon 27a. Single-stranded DNA samples were electrophoresed in 6% acrylamide [75:1] on the EC 160 apparatus at 45 W constant power at 4°C for 8 hours. Phosphorimager exposure was 36 hours. Lanes: mother (M), father (F), child (C), and wild-type control (WT).

3.5.2. Low pH SSCP Protocol

A modified protocol (number 4) (5% acrylamide in TPE [pH 6.8]) was applied to enhance the mutation detection efficiency of SSCP for the longer DNA fragments, *NF1* exons 16 and 23a. Altered mobilities were detected for both the positive control and the child's *NF1* exon 22 DNA fragment using this protocol (data not shown). However, no difference between the mobility of the child's DNA and the control DNA fragments was seen for *NF1* exons 16 or 23a (Figure 3.9). Both digested and undigested PCR products of exons 16 and 23a were analyzed using this protocol.

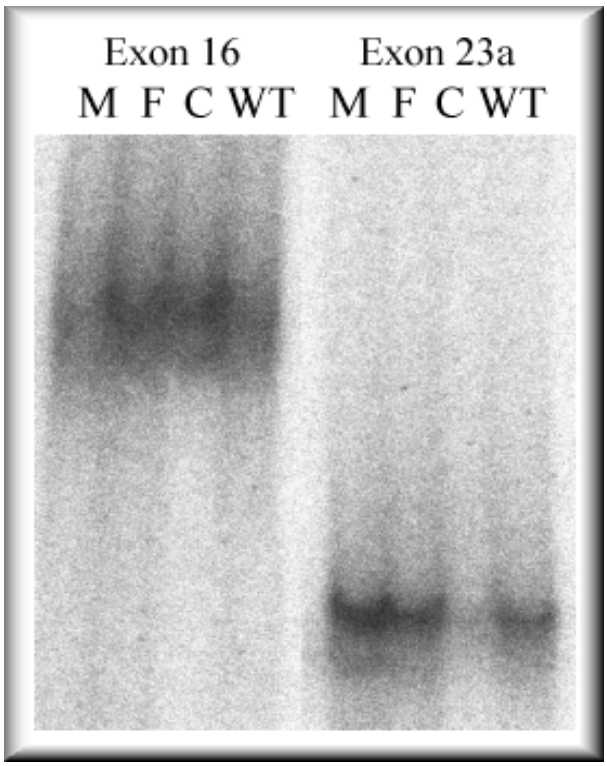

Figure 3.9. Low pH SSCP analysis of *NF1* exon 16 and *NF1* exon 23a. Single-stranded DNA fragments were electrophoresed in 5% [99:1] acrylamide on the EC 160 apparatus at 40 W constant power at 4°C for 3 hours]. Phosphorimager exposure was 36 hours. Lanes: mother (M), father (F), child (C), and wild-type control (WT).

3.6. DNA Sequence Analysis

In order to pinpoint the cause of the altered mobility observed for *NF1* exon 22, DNA sequence analysis was performed. Cycle sequencing reactions were carried out using intronic primers for exon 22 (Table 2.1). Gel electrophoresis of the cycle sequencing reaction products revealed a heterozygous C→T transition at nucleotide position 3721 in child's sample (Figure 3.10, panel a). This mutation results in the substitution of a stop codon instead of the arginine codon at residue position 1241 and truncation of the protein at the beginning of its functional GRD domain. The truncated neurofibromin is expected to lack its GTPase activating function. Repeat

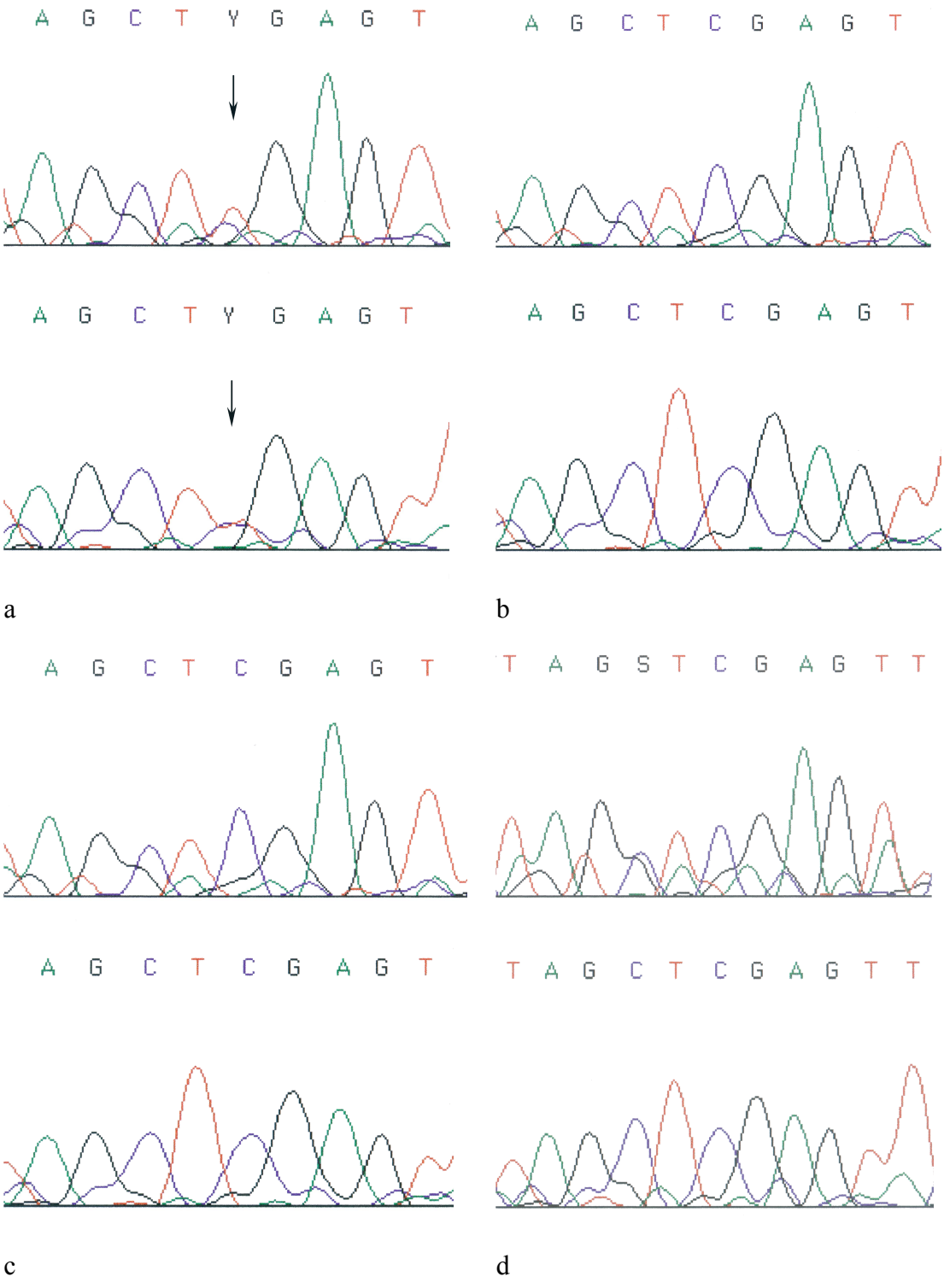

Figure 3.10. DNA sequence analysis of *NF1* exon 22. a. Child (IV-4). **b.** Mother (III-5). **c.** Father (III-6). **d.** Sibling (IV-3). Each panel shows the nucleotide sequence obtained with forward (upper) and reverse (lower) primers. Arrow indicates heterozygosity [T/C designated as Y] at nucleotide 3721.

analysis of an independent PCR product yielded the same results (data not shown). This mutation was not found in the mother, father or sibling (Figure 3.10, panels b-d), suggesting that two independent *de novo* mutations were responsible for the signs and symptoms of neurofibromatosis observed in the two children.

3.7. Mutation Verification by *Taq*I Digestion

Since the C1241T transition results in loss of the *Taq*I restriction site (TCGA→TTGA), we performed *Taq*I restriction enzyme digestion to confirm the mutation. In a wild-type individual (TCGA), we would expect to see two DNA fragment bands (245 + 86 bp) after *Taq*I digestion. In an individual homozygous for the C→T mutation, the restriction site would be lost and as a result only one DNA fragment band would be seen after *Taq*I digestion. In a heterozygous individual, *Taq*I restriction would result in three bands: the uppermost band (331 bp) representing the mutant allele lacking the *Taq*I site; and the middle and lower bands (245 + 86 bp) representing the wild-type allele with its *Taq*I restriction site.

*Taq*I digestion of the *NF1* exon 22 PCR product of the child resulted in three DNA fragments (Figure 3.11), confirming heterozygosity in the child's sample due to loss of *Taq*I restriction site in the mutant allele. *Taq*I digestion of the *NF1* exon 22 PCR product of the mother, father and sibling revealed only two DNA fragments (Figure 3.11), thus, confirming the presence of the wild-type sequence in both alleles.

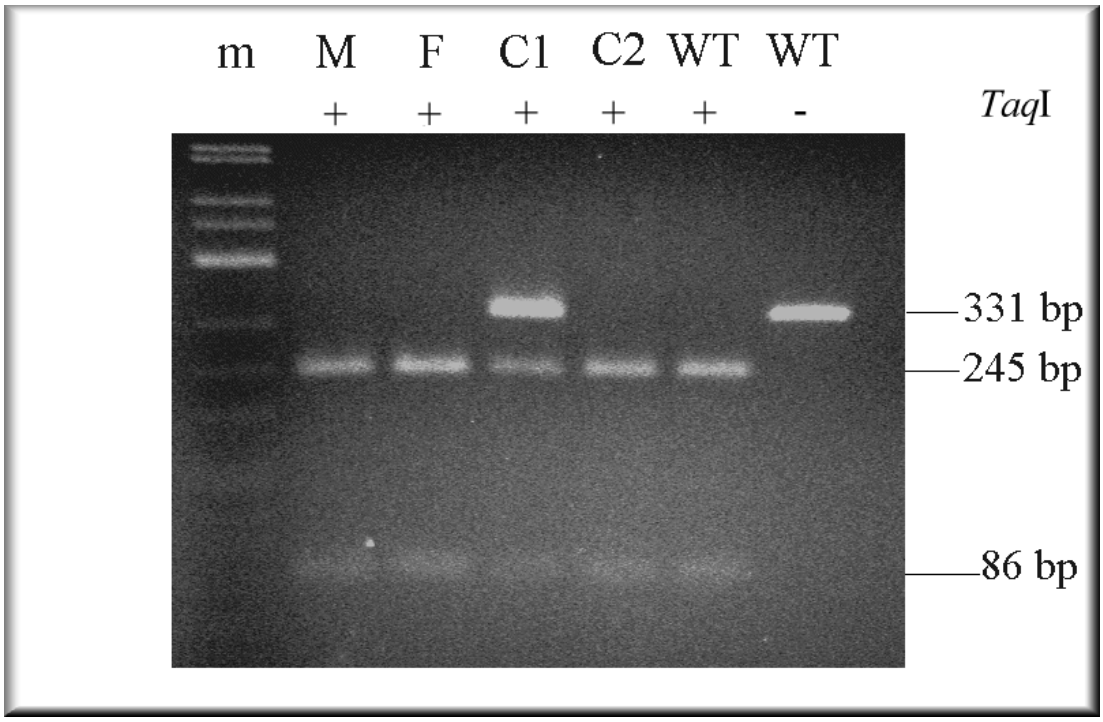

Figure 3.11. Mutation verification by *Taq*I restriction digest. *Taq*I-digested DNA was electrophoresed in 4% NuSieve 3:1 agarose at 50V for 3 hours. Lanes with "+" sign contain *Taq*I-digested samples, while the lane with a "-" sign contains an undigested control sample. Fragment sizes are shown in the right margin. Lanes: ΦX174/*Hae*III molecular weight marker (m), mother (M), father (F), child IV-4 (C1), sibling IV-3 (C2), wild-type control (WT).

3.8. Allele-specific Amplification of *MLH1*

Since the sibling's DNA had been isolated form a bone morrow smear, which was not preserved under pristine conditions, the sample had to be checked for possible wild-type DNA contamination. As previously shown, the sibling was homozygous for a C676T mutation in *MLH1* exon 8 (Ricciardone *et al.*, 1999). Allele-specific amplification (Gibbs *et al.*, 1989) would be a powerful tool to determine the genotype of this sample and confirm that it had not been contaminated with wild-type DNA. In this assay, allele-specific primers differing only at the 3' terminal nucleotide were designed to specifically amplify either the wild-type allele

or mutant allele. After PCR amplification, we would expect to see only the wild-type allele amplified from a wild-type individual; both alleles amplified from a heterozygous individual; and only the mutant allele amplified from a homozygous individual.

Allele-specific amplification using specific primers for the wild-type and mutant alleles for *MLH1* exon 8 was performed for the child, sibling, father, and a wild-type control DNA. When either the child's DNA or the sibling's DNA was used as a template, PCR products were obtained only when the mutant allele-specific primers were used (Figure 3.12, lanes 1 and 2). When the father's DNA was used as a template, PCR products were obtained with either the wild-type or mutant allele-specific primers (Figure 3.12, lane 3). When wild-type DNA was used as a template, PCR products were obtained only when the wild-type allele-specific primers were used (Figure 3.12, lane 4).

The sensitivity of this technique is high enough to detect the presence of one mutant allele among 50 copies of the wild-type allele (Ricciardone *et al.*, 1999). Since these results match previously published results (Ricciardone *et al.*, 1999), they confirm the lack of wild-type DNA contamination in the sibling DNA sample. Thus, the inability to detect the C3721T *NF1* mutation in the sibling is not due to contamination of sibling DNA with wild-type DNA, but rather reflects the absence of that mutation in the sibling.

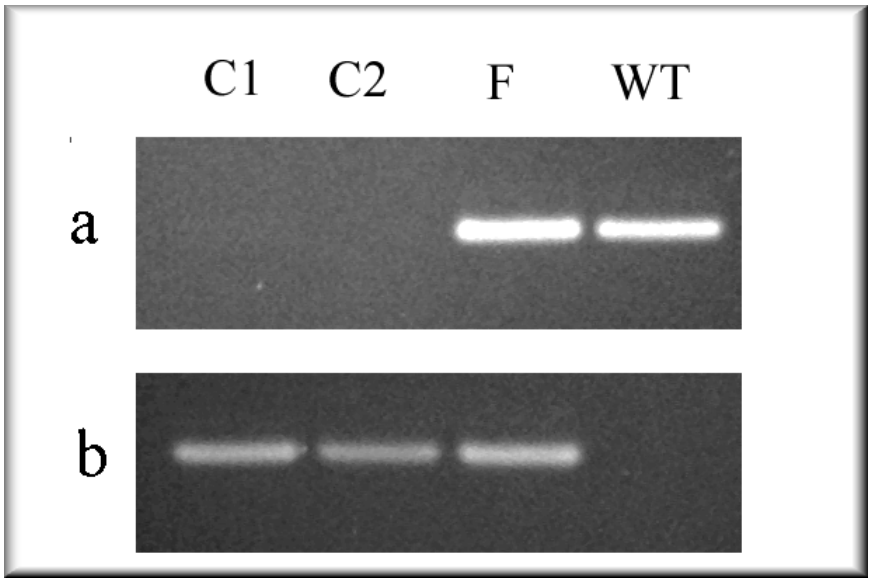

Figure 3.12. Allele specific amplification analysis. a. PCR products amplified with wild-type-specific primer. **b.** PCR products amplified with mutant-specific primer. Lanes: child IV-4 (C1), sibling IV-3 (C2) father (F), wild-type control (WT).

4. DISCUSSION

HNPCC is a relatively common hereditary disease that affects approximately 1 in 200 to 1,000 individuals and accounts for 3% of all colorectal cancers (Boland, 1998). Defects in five DNA mismatch repair genes, *MLH1*, *MSH2*, *PMS1*, *PMS2*, and *MSH6*, have been linked to HNPCC, with the majority of the mutations occurring in *MLH1* and *MSH2* (Papadopoulos and Lindblom, 1997). Individuals with a germ line mutation in one of these DNA mismatch repair genes have greater risk of developing colorectal cancer.

HNPCC tumorigenesis is a multi-step process. The first step involves inheritance of a germ line mutation in one of the DNA mismatch repair genes. These individuals have apparently normal DNA MMR due to the presence of a wild-type allele and functional gene product (Tannergard *et al.*, 1997). The second step involves somatic mutation of the wild-type allele. With two mutant alleles, there is no functional gene product and DNA mismatch repair deficiency occurs. Progeny cells have a mutator phenotype that is evidenced by microsatellite instability (Aaltonen *et al.*, 1993). The third step involves a somatic downstream mutation in a cellular growth control gene. Downstream mutations in HNPCC individuals have been reported for *TGFβRII* (Markowitz *et al.*, 1995), *IGFRII* (Souza *et al.*, 1996), *BAX* (Rampino *et al.*, 1997), and *MSH3* and *MSH6* (Yamamoto *et al.*, 1998). These

mutations give the affected cells a growth advantage that has been implicated in the progression of colorectal cancer.

Although the consequence of heterozygous germ line mutations and subsequent somatic loss of DNA mismatch repair function have been well characterized, the phenotypic consequence of constitutional loss of DNA MMR gene function is poorly understood. Recently, a homozygous *MLH1* mutation [C676T] that results in a severely truncated nonfunctional protein [Arg226Stop] was identified in two offspring of heterozygous consanguineous parents, both afflicted with colorectal cancer (Ricciardone *et al.*, 1999). This mutation results in a truncated, nonfunctional protein and probable DNA mismatch repair deficiency. Both offspring showed an unusual phenotype not previously observed in HNPCC kindreds -- neurofibromatosis type 1 and an early onset of hematological malignancy. We hypothesized that, in these individuals, the homozygous *MLH1* mutation resulted in a complete DNA mismatch repair deficiency in all cells and that a downstream mutation in *NF1* was responsible for the unusual phenotype.

The aim of this study was to identify the putative *NF1* gene mutation and, ultimately, clarify the genetic mechanism involved in this phenotype. A strategy for mutation detection was defined so that the analysis of the very large *NF1* coding region (8454 bp) would be logical and affordable. The strategy involved, first, identification of *NF1* mutation hot spots, such as microsatellites and CpG islands in the *NF1* coding region. Second step involved designing intronic primers to amplify the targeted exons. Third step involved SSCP analysis of the targeted exons in the child's genomic DNA for altered mobility that might indicate a causative mutation.

The final step involved DNA sequence analysis of those exons with altered SSCP mobility to identify the cause of the altered mobility and verify the putative mutation.

Microsatellites are potential mutation hot spots in DNA mismatch repair deficient cells because of the potential for DNA polymerase slippage (Trinh and Sinden, 1991). The *NF1* coding region contains 36 microsatellites in 26 different exons. These exons were prioritized as follows: first priority was given to the five exons within the NF1 GAP-related domain, since a mutation in this region would destroy the GTPase activating function of the protein; second priority was given to exon 29 because of the multiple CpG islands that are known to be mutation hot spots (Rodenhiser *et al.*, 1997); third priority was give to for exons containing mononucleotide repeat motifs, followed by those containing dinucleotide, and finally trinucleotide repeat motifs.

Intronic primer sequences that had been successfully used by more than one research group (Li *et al.*, 1995; Maynard *et al.*, 1997; Upadhyaya *et al.*, 1997; Abernathy *et al.*, 1997) were selected for PCR amplification. PCR parameters were optimized so produce a single DNA fragment with no extraneous nonspecific amplification. The target exons were amplified by radioactive PCR and analyzed by SSCP, using previously optimized protocols (Akyerli, MSc thesis, 1998). Multiple SSCP protocols were necessary for maximal mutation detection since the sensitivity of this technique is less than 100%. Alternative protocols were applied to enhance mutation detection in two exons longer than 500 bp. First, restriction digestion of exon 16 by *Eco*RII and exon 23a by *Hin*fI results in smaller fragment sizes within the range of conventional SSCP analysis. Second, a low pH SSCP protocol designed to

detect mutations in DNA fragments as long as 800 bp (Kukita *et al.*, 1997) was used to analyze these exons.

SSCP analysis of the child's genomic DNA revealed an altered mobility for *NF1* exon 22 compared to the parental DNA samples. SSCP analysis of exons 16, 21, 23-2, 23a, and 27 revealed no altered mobility using any of the protocols. DNA sequence analysis of *NF1* exon 22 revealed that the altered SSCP mobility was due to a heterozygous C to T transition at nucleotide 3721. This mutation results in the substitution of a stop signal for an arginine residue at codon position 1241. Structurally, codon 1241 is located in the first extra domain of the neurofibromin GRD. This mutation, therefore, would result in a truncated protein lacking the GTPase activating function. Furthermore, all functional domains encoded by the more C terminal coding region will also be missing.

DNA sequence analysis of *NF1* exon 22 in other family members (mother, father and sibling) showed no mutation. The point mutation was verified by restriction enzyme digestion with *Taq*I, whose restriction site is lost as a consequence of the C→T transition. The presence of three restriction fragments confirmed the heterozygosity of the child for this mutation, while the presence of two restriction fragments in the other family members (mother, father and sibling) confirmed their wild-type status.

Although many mutations observed in DNA mismatch repair deficient cells have been found in homopolymeric tracts, downstream mutations are not necessarily limited to these sequences. The *NF1* C3721T transition defined in this study did not occur in a microsatellite repeat motif but, rather, in a CpG dinucleotide. CpG

dinucleotides are also considered mutation hot spots in the human genome. These islands are susceptible modification at the 5' cytosine by cellular DNA methyltransferases. Spontaneous deamination of 5-methyl cytosine (5mC) to thymidine occurs at very high frequency, thus, contributing significantly to the incidence of human genetic diseases (Cooper and Krawczak, 1989).

In order to verify that the negative DNA sequence analysis and negative *Taq*I digestion of the sibling's DNA sample was not due to wild-type DNA contamination, the sibling's *MLH* genotype was determined by allele-specific amplification of *MLH* exon 8. This experiment confirmed that all family members' DNA samples were of the expected genotype. Specifically, the parents were heterozygous and both children were homozygous for the *MLH1* exon 8 alleles. Thus, the sibling's DNA sample was not contaminated with wild-type DNA that might have masked the presence of the mutation in *NF1* exon 22.

The presence of this germ line *NF1* mutation in only one of the two offspring homozygous for the *MLH1* mutation and afflicted with neurofibromatosis type I and hematological malignancy suggests that this mutation was not inherited from either parent but was rather a *de novo* mutation. *NF1* has one of the highest mutation rates (Shen *et al.*, 1996) and, thus, would be a likely target for a spontaneous mutation. Since the mutation is present in the germ line, it most likely occurred during the early stages of embryonic development.

As *NF1* is a tumor suppressor gene (Sawada *et al.*, 1996), a putative second somatic mutation most likely occurred in the wild-type allele and caused loss of neurofibromin function. Neurofibromin plays a crucial role in regulating Ras

activity, catalyzing the conversion of the active Ras•GTP to the inactive Ras•GDP. Loss of neurofibromin would result in decreased GAP activity and high levels of activated Ras•GTP, which would result in increased cell proliferation and tumor formation.

Perspectives

This study focused on a child with a homozygous germ line mutation in *MLH1* [C676T→Arg226Stop] inherited from consanguineous parents (Ricciardone *et al.*, 1999). This child presented with neurofibromatosis type 1 and hematological malignancy, instead of the colorectal cancer phenotype usually seen in HNPCC individuals. This study identified a heterozygous germ line mutation in the *NF1* gene that results in truncation of the *NF1* gene product at the beginning of the functional GTPase activation domain. Impaired regulation of Ras•GTP signaling probably contributed to the tumor development in this child.

The unusual association of HNPCC with neurofibromatosis and early childhood hematological malignancy has also been observed in an HNPCC kindred from North Africa (Wang *et al.*, 1999), in which the affected child was homozygous for a germ line *MLH1* mutation inherited from heterozygous parents. These two independent observations suggest that, in the presence of genetic instability, such as constitutional DNA mismatch repair deficiency, the *NF1* gene is a preferential target for downstream mutations, probably because of the high mutation rate observed at the *NF1* locus (Shen *et al.*, 1996).

Somatic loss of DNA MMR activity in HNPCC patients has been associated with downstream mutations growth control genes such as *TGFβRII*, *IGFIIR*, *BAX*, *MSH3* and *MSH6* (Markowitz *et al.*, 1995; Souza *et al.*, 1996; Rampino *et al.*, 1997; Yamamoto *et al.*, 1998). However, clinical evidence suggested that constitutional loss of DNA MMR activity in HNPCC individuals due to homozygous mutations in *MLH1* would be associated with downstream mutations in *NF1*, another gene involved in growth control regulation. The identification of a germline truncating mutation in *NF1* in this study provides strong genetic evidence in support of that hypothesis. The resulting impaired regulation of Ras•GTP signaling contributed to tumor development --neurofibromatosis type 1 and hematological malignancy.

Heterozygous mice with a germ-line mutation in *NF1* do not exhibit classical symptoms of human neurofibromatosis. However, they do develop a variety of tumors, including phaeochromocytoma and myeloid leukemia, both of which occur with high frequency in NF1 patients (Jacks *et al.*, 1996). Studies using other mouse models have demonstrated that constitutional DNA MMR deficiency results in high levels of DNA replication errors *in vivo* and high levels of spontaneous tumor development. *Mlh1*-deficient mice succumbed to lymphoma before 30 weeks and died before one year of age (Reitmair *et al.*, 1996; de Wind *et al.*, 1998). Mice deficient for *Msh2* and *Pms2* also developed lymphomas and died at early age (Prolla *et al.*, 1998; Edelmann *et al.*, 1999). Although the MMR-deficient mice apparently do not develop neurofibromatosis, they do develop hematological malignancies. Thus, it would be interesting to search for *NF1* mutations in these MMR-deficient mice to determine whether a similar genetic cascade occurs in mice. It would also be

interesting to develop an *Mlh1*$^{-/-}$ / *Nf1*$^{+/-}$ hybrid mouse strain and observe the resulting phenotype. Such studies in animals might give further insights into the development of human disease.

REFERENCES

Aaltonen, L. A., Peltomaki, P., Leach, F. S., Sistonen, P., Pylkkanen, L., Mecklin, J. P., Jarvinen, H., Powell, S. M., Jen, J., Hamilton, S. R., Peterson, G. M., Kinzler, K. W., Vogelstein, B., and de la Chapelle, A. Clues to the pathogenesis of familial colorectal cancer. *Science* **260**: 812-816, 1993.

Abernathy, C. R., Rasmussen, S. A., Stalker, H. J., Zori, R., Driscoll, D. J., Williams, C. A., Kousseff, B. G., and Wallace, M. R. *NF1* mutation analysis using a combined heteroduplex/SSCP approach. *Hum. Mutat.* **9**: 548-554, 1997.

Akiyama, Y., Sato, H., Yamada, T., Nagasaki, H., Tsuchiya, A., Abe, R., and Yuasa, Y. Germ-line mutation of the *hMSH6*/*GTBP* gene in an atypical hereditary nonpolyposis colorectal cancer kindred. *Cancer Res.* **57**: 3920-3923, 1997a.

Akiyama, Y., Tsubouchi, N., and Yuasa, Y. Frequent somatic mutations of *hMSH3* with reference to microsatellite instability in hereditary nonpolyposis colorectal cancers. *Biochem. Biophys. Res. Commun.* **236**: 248-252, 1997b.

Akyerli, C. Analysis of *hMLH1* germline mutations in three Turkish hereditary nonpolyposis colorectal cancer kindreds. Bilkent University, MSc. Thesis, 1998.

Anglani, F., Murgia, A., Bedin, S., Bresin, E., Bernardi, F., Clementi, M., and Tenconi, R. A new disease-causing mutation in the GAP-related domain of the *NF1* gene. *Hum. Mol. Genet.* **2**: 1057-1059, 1993.

Arzimanoglou, I. I., Gilbert, F., and Barber, H. R. Microsatellite instability in human solid tumors. *Cancer* **82**: 1808-1820, 1998.

Ashkenas, J. Gene regulation by mRNA editing. *Am. J. Hum. Genet.* **60**: 278-283, 1997.

Backus, J. W. and Smith, H. C. Apolipoprotein B mRNA sequences 3' of the editing site are necessary and sufficient for editing and editosome assembly. *Nucleic Acids Res.* **19**: 6781-6786, 1991.

Ballester, R., Marchuk, D., Boguski, M., Saulino, A., Letcher, R., Wigler, M., and Collins, F. The *NF1* locus encodes a protein functionally related to mammalian GAP and yeast IRA proteins. *Cell* **63**: 851-859, 1990.

Behrens, J., von Kries, J. P., Kuhl, M., Bruhn, L., Wedlich, D., Grosschedl, R., Birchmeier, W. Functional interaction of beta-catenin with the transcription factor LEF-1. *Nature* **382**: 638-642, 1996.

Bellacosa, A., Cicchillitti, L., Schepis, F., Riccio, A., Yeung, A. T., Matsumoto, Y., Golemis, E. A., Genuardi, M., and Neri, G. MED1, a novel human methyl-CpG-binding endonuclease, interacts with DNA mismatch repair protein MLH1. *Proc. Natl. Acad. Sci. U.S.A.* **96**: 3969-74, 1999.

Boland, C.R. Hereditary nonpolyposis colorectal cancer. In: Vogelstein, B., Kinzler, K. W., editors. *The Genetic Basis of Human Cancer*. New York: McGraw-Hill, pp. 333-346, 1998.

Bollag, G., McCormick, F., and Clark, R. Characterization of full-length neurofibromin: tubulin inhibits Ras GAP activity. *Embo J.* **12**: 1923-1927, 1993.

Bronner, C. E., Baker, S. M., Morrison, P. T., Warren, G., Smith, L. G., Lescoe, M. K., Kane, M., Earabino, C., Lipford, J., Lindblom, A., Tannergard, P., Bollag, R. J., Godwin, A. R., Ward, D. C., Nordenskjold, M., Fishel, R., Kolodner, R., and Liskay, R. M. Mutation in the DNA mismatch repair gene homologue *hMLH1* is associated with hereditary non-polyposis colon cancer. *Nature* **368**: 258-261, 1994.

Buchberg, A. M., Cleveland, L. S., Jenkins, N. A., and Copeland, N. G. Sequence homology shared by neurofibromatosis type-1 gene and IRA-1 and IRA-2 negative regulators of the RAS cyclic AMP pathway. *Nature* **347**: 291-294, 1990.

Cappione, A. J., French, B. L., and Skuse, G. R. A potential role for *NF1* mRNA editing in the pathogenesis of NF1 tumors. *Am. J. Hum. Genet.* **60**: 305-312, 1997.

Cawthon, R. M., Andersen, L. B., Buchberg, A. M., Xu, G. F., O'Connell, P., Viskochil, D., Weiss, R. B., Wallace, M. R., Marchuk, D. A., Culver, M., Stevens, J., Jenkins, N., Copeland, N., Collins, F., and White, R. cDNA sequence and genomic structure of EV12B, a gene lying within an intron of the neurofibromatosis type 1 gene. *Genomics* **9**: 446-460, 1991.

Cawthon, R. M., Weiss, R., Xu, G. F., Viskochil, D., Culver, M., Stevens, J., Robertson, M., Dunn, D., Gesteland, R., O'Connell, P., and White, R. A major segment of the neurofibromatosis type 1 gene: cDNA sequence, genomic structure, and point mutations [published erratum appears in Cell 62: 608, 1990]. *Cell* **62**: 193-201, 1990.

Cooper, D. N. and Krawczak, M. Cytosine methylation and the fate of CpG dinucleotides in vertebrate genomes. *Hum. Genet.* **83**: 181-8, 1989.

Cummings, L. M., Glatfelter, A., and Marchuk, D. A. *NF1*-related loci on chromosome 2, 12, 14, 15, 20, and 22: a potential role for gene conversion in the high spontaneous mutation rate of *NF1*? *Am. J. Hum. Genet.* **53**(suppl): 672, 1993.

Danglot, G., Regnier, V., Fauvet, D., Vassal, G., Kujas, M., and Bernheim, A. Neurofibromatosis 1 (NF1) mRNAs expressed in the central nervous system are differentially spliced in the 5' part of the gene. *Hum. Mol. Genet.* **4**: 915-920, 1995.

de Wind, N., Dekker, M., van Rossum, A., van der Valk, M., and te Riele, H. Mouse models for hereditary nonpolyposis colorectal cancer. *Cancer Res.* **58**: 248-255, 1998.

DeClue, J. E., Cohen, B. D., and Lowy, D. R. Identification and characterization of the neurofibromatosis type 1 protein product. *Proc. Natl. Acad. Sci. U.S.A.* **88**: 9914-9918, 1991.

Dietmaier, W., Wallinger, S., Bocker, T., Kullmann, F., Fishel, R., and Ruschoff, J. Diagnostic microsatellite instability: definition and correlation with mismatch repair protein expression. *Cancer Res.* **57**: 4749-4756, 1997.

Drummond, J. T., Li, G. M., Longley, M. J., and Modrich, P. Isolation of an hMSH2-p160 heterodimer that restores DNA mismatch repair to tumor cells. *Science* **268**: 1909-1912, 1995.

Edelmann, W., Yang, K., Kuraguchi, M., Heyer, J., Lia, M., Kneitz, B., Fan, K., Brown, A. M., Lipkin, M., and Kucherlapati, R. Tumorigenesis in *Mlh1* and *Mlh1/Apc1638N* mutant mice. *Cancer Res.* **59**: 1301-1307, 1999.

Eshleman, J. R. and Markowitz, S. D. Mismatch repair defects in human carcinogenesis. *Hum. Mol. Genet.* **5**: 1489-1494, 1996.

Fink, D., Nebel, S., Aebi, S., Zheng, H., Kim, H. K., Christen, R. D., and Howell, S. B. Expression of the DNA mismatch repair proteins hMLH1 and hPMS2 in normal human tissues. *Br. J. Cancer.* **76**: 890-3, 1997.

Fishel, R. Mismatch repair, molecular switches, and signal transduction. *Genes Dev.* **12**: 2096-2101, 1998.

Fishel, R., Lescoe, M. K., Rao, M. R., Copeland, N. G., Jenkins, N. A., Garber, J., Kane, M., and Kolodner, R. The human mutator gene homolog MSH2 and its association with hereditary nonpolyposis colon cancer [published erratum appears in Cell 77: 167, 1994]. *Cell* **75**: 1027-1038, 1993.

Garty, B. Z., Laor, A., and Danon, Y. L. Neurofibromatosis type 1 in Israel: survey of young adults. *J. Med. Genet.* **31**: 853-857, 1994.

Gibbs, R. A., Nguyen, P. N., and Caskey, C. T. Detection of single DNA base differences by competitive oligonucleotide priming. *Nucleic Acids Res.* **17**: 2437-2448, 1989.

Goldberg, N. S. and Collins, F. S. The hunt for the neurofibromatosis gene. *Arch. Dermatol.* **127**: 1705-1707, 1991.

Gradia, S., Acharya, S., and Fishel, R. The human mismatch recognition complex hMSH2-hMSH6 functions as a novel molecular switch. *Cell* **91**: 995-1005, 1997.

Gradia, S., Subramanian, D., Wilson,T., Acharya, S., Makhov, A., Griffith, J., and Fishel, R. hMSH2-hMSH6 forms a hydrolysis-independent sliding clamp on mismatched DNA. *Mol. Cell.* **3**: 255-61, 1999.

Grifa, A., Piemontese, M. R., Melchionda, S., Origone, P., Zelante, L., Coviello, D., Fratta, G., Dallapiccola, B., Balestrazzi, P., Ajmar, F., and Gasparini, P.

Screening of neurofibromatosis type 1 gene: identification of a large deletion and of an intronic variant. *Clin. Genet.* **47**: 281-284, 1995.

Groden, J., Thliveris, A., Samowitz, W., Carlson, M., Gelbert, L., Albertsen, H., Joslyn, G., Stevens, J., Spirio, L., and Robertson, M. Identification and characterization of the familial adenomatous polyposis coli gene. *Cell* **66**: 589-600, 1991.

Grompe, M. The rapid detection of unknown mutations in nucleic acids. *Nat. Genet.* **5**: 111-117, 1993.

Gryfe, R., Swallow, C., Bapat, B., Redston, M., Gallinger, S., and Couture, J. Molecular biology of colorectal cancer. *Curr. Probl. Cancer* **21**: 233-300, 1997.

Guatelli, J. C., Whitfield, K. M., Kwoh, D. Y., Barringer, K. J., Richman, D. D., and Gingeras, T. R. Isothermal, in vitro amplification of nucleic acids by a multienzyme reaction modeled after retroviral replication [published erratum appears in Proc. *Natl. Acad. Sci. U.S.A* 19: 7797,1990]. *Proc. Natl. Acad. Sci. U.S.A.* **87**: 1874-8, 1990.

Gutmann, D. H., Andersen, L. B., Cole, J. L., Swaroop, M., and Collins, F. S. An alternatively-spliced mRNA in the carboxy terminus of the neurofibromatosis type 1 (*NF1*) gene is expressed in muscle. *Hum. Mol. Genet.* **2**: 989-992, 1993.

Gutmann, D. H., Geist, R. T., Wright, D. E., and Snider, W. D. Expression of the neurofibromatosis 1 (*NF1*) isoforms in developing and adult rat tissues. *Cell Growth Differ.* **6**: 315-323, 1995.

Gutmann, D. H., Wood, D. L., and Collins, F. S. Identification of the neurofibromatosis type 1 gene product. *Proc. Natl. Acad. Sci. U.S.A.* **88**: 9658-9662, 1991.

Hayashi, K., PCR-SSCP: Single-strand conformation polymorphism analysis of PCR products. In: *Laboratory Protocols For Mutation Detection, Edited by Ulf Landegren*., Oxford Uni. Press, Chapter 4, 1996.

Hayashi, K. and Yandell, D. W. How sensitive is PCR-SSCP? *Hum. Mutat.* **2**: 338-346, 1993.

He, T. C., Sparks, A.B., Rago, C., Hermeking, H., Zawel, L., da Costa, L. T., Morin, P. J., Vogelstein, B., Kinzler, K. W. Identification of c-MYC as a target of the APC pathway. *Science* **281**: 1509-1512, 1998.

Heim, R. A., Kam-Morgan, L. N., Binnie, C. G., Corns, D. D., Cayouette, M. C., Farber, R. A., Aylsworth, A. S., Silverman, L. M., and Luce, M. C. Distribution of 13 truncating mutations in the neurofibromatosis 1 gene. *Hum. Mol. Genet.* **4**: 975-981, 1995.

Huson, S. M., Compston, D. A., Clark, P., and Harper, P. S. A genetic study of von Recklinghausen neurofibromatosis in south east Wales. I. Prevalence, fitness, mutation rate, and effect of parental transmission on severity. *J. Med. Genet.* **26**: 704-711, 1989.

Hutter, P., Antonarakis, S. E., Delozier-Blanchet, C. D., and Morris, M. A. Exon skipping associated with A→G transition at +4 of the IVS33 splice donor site of the neurofibromatosis type 1 (*NF1*) gene. *Hum. Mol. Genet.* **3**: 663-5, 1994.

Ichii, S., Horii, A., Nakatsuru, S., Furuyama, J., Utsunomiya, J., and Nakamura, Y. Inactivation of both APC alleles in an early stage of colon adenomas in a patient with familial adenomatous polyposis (FAP). *Hum. Mol. Genet.* **1**: 387-390, 1992.

Jacks, T., Shih, S., Schmitt, E. M., Bronson, R. T., Bernards, A. and Weinberg, R. A. Tumor predisposition in mice heterozygous for a targeted mutation in *Nf1*. *Nature Genet.* **7**: 353-361, 1996.

Joslyn, G., Carlson, M., Thliveris, A., Albertsen, H., Gelbert, L., Samowitz, W., Groden, J., Stevens, J., Spirio, L., Robertson, M., *et al.* Identification of deletion mutations and three new genes at the familial polyposis locus. *Cell* **66**: 601-613, 1991.

Kinzler, K. W. and Vogelstein, B. Lessons from hereditary colorectal cancer. *Cell* **87**: 159-170, 1996.

Kinzler, K. W., Nilbert, M. C., Su, L. K., Vogelstein, B., Bryan, T. M., Levy, D. B., Smith, K. J., Preisinger, A. C., Hedge, P., and McKechnie, D. Identification of FAP locus genes from chromosome 5q21. *Science* **253**: 661-665, 1991.

Knudson, A. G. Anti-oncogenes and human cancer. *Proc. Natl. Acad. Sci. U.S.A.* **90**: 10914-10921, 1993.

Kolodner, R. Biochemistry and genetics of eukaryotic mismatch repair. *Genes Dev.* **10**: 1433-1442, 1996.

Kolodner, R. D. Mismatch repair: mechanisms and relationship to cancer susceptibility. *Trends Biochem. Sci.* **20**: 397-401, 1995.

Krawczak, M. and Cooper, D. N. The human gene mutation database. *Trends Genet.* **13**: 121-2, 1997.

Kukita, Y., Tahira, T., Sommer, S. S., and Hayashi, K. SSCP analysis of long DNA fragments in low pH gel. *Hum. Mutat.* **10**: 400-407, 1997.

Lahue, R. S., Au, K. G., and Modrich, P. DNA mismatch correction in a defined system. *Science* **245**: 160-164, 1989.

Lazaro, C., Ravella, A., Gaona, A., Volpini, V., and Estivill, X. Neurofibromatosis type 1 due to germ-line mosaicism in a clinically normal father. *N. Engl. J. Med.* **331**: 1403-1407, 1994.

Leach, F. S., Nicolaides, N. C., Papadopoulos, N., Liu, B., Jen, J., Parsons, R., Peltomaki, P., Sistonen, P., Aaltonen, L. A., Nystrom-Lahti, M., Guan, X.-Y., Zhang, J., Meltzer, P. S., Yu, J.-W., Kao, F.-T., Chen, D. J., Cerosaletti, K. M., Fournier, R. E. K., Todd, S., Lewis, T., Leach, R. J., Naylor, S. L., Weissenbach, J., Mecklin, J.-P., Jarvinen, H., Peterson, G. M., Hamilton, S. R., Green, J., Jass, J., Watson, P., Lynch, H. T., Trent, J. M., de la Chapelle, A., Kinzler, K. W., and Vogelstein, B. Mutations of a mutS homolog in hereditary nonpolyposis colorectal cancer. *Cell* **75**: 1215-1225, 1993.

Levy, D. B., Smith, K. J., Beazer-Barclay, Y., Hamilton, S. R., Vogelstein, B., and Kinzler, K. W. Inactivation of both APC alleles in human and mouse tumors. *Cancer Res.* **54**: 5953-5958, 1994.

Li, Y., O'Connell, P., Breidenbach, H. H., Cawthon, R., Stevens, J., Xu, G., Neil, S., Robertson, M., White, R., and Viskochil, D. Genomic organization of the neurofibromatosis 1 gene (*NF1*). *Genomics* **25**: 9-18, 1995.

Lindahl, T., Karran, P., and Wood, R. D. DNA excision repair pathways. *Curr. Opin. Genet. Dev.* **7**: 158-169, 1997.

Lindblom, A., Tannergard, P., Werelius, B., and Nordenskjold, M. Genetic mapping of a second locus predisposing to hereditary non- polyposis colon cancer. *Nat. Genet.* **5**: 279-282, 1993.

Littler, M. and Morton, N. E. Segregation analysis of peripheral neurofibromatosis (NF1). *J. Med. Genet.* **27**: 307-310, 1990.

Lott, I. T. and Richardson, E. P., Jr. Neuropathological findings and the biology of neurofibromatosis. *Adv. Neurol.* **29**: 23-32, 1981.

Lynch, H. T. and Smyrk, T. Hereditary nonpolyposis colorectal cancer (Lynch syndrome): An updated review. *Cancer* **78**: 1149-1167, 1996.

Lynch, H. T., Smyrk, T. C., Watson, P., Lanspa, S. J., Lynch, J. F., Lynch, P. M., Cavalieri, R. J., and Boland, C. R. Genetics, natural history, tumor spectrum, and pathology of hereditary nonpolyposis colorectal cancer: An updated review. *Gastroenterology* **104**: 1535-1549, 1993.

Lynch, H. T., Smyrk, T., and Lynch, J. F. Overview of natural history, pathology, molecular genetics and management of HNPCC (Lynch Syndrome). *Int. J. Cancer* **69**: 38-43, 1996.

Marchuk, D. A., Saulino, A. M., Tavakkol, R., Swaroop, M., Wallace, M. R., Andersen, L. B., Mitchell, A. L., Gutmann, D. H., Boguski, M., and Collins, F. S. cDNA cloning of the type 1 neurofibromatosis gene: complete sequence of the *NF1* gene product. *Genomics* **11**: 931-940, 1991.

Markowitz, S., Wang, J., Myeroff, L., Parsons, R., Sun, L., Lutterbaugh, J., Fan, R. S., Zborowska, E., Kinzler, K. W., Vogelstein, B., Brattian, M., and Willson, J. K. V. Inactivation of the type II TGF-beta receptor in colon cancer cells with microsatellite instability. *Science* **268**: 1336-1338, 1995.

Maynard, J., Krawczak, M., and Upadhyaya, M. Characterization and significance of nine novel mutations in exon 16 of the neurofibromatosis type 1 (*NF1*) gene. *Hum. Genet.* **99**: 674-676, 1997.

McCormick, F. Ras signaling and NF1. *Curr Opin Genet Dev* **5**: 51-55, 1995.

Mecklin, J. P., Jarvinen, H. J., Hakkiluoto, A., Hallikas, H., Hiltunen, K. M., Harkonen, N., Kellokumpu, I., Laitinen, S., Ovaska, J., and Tulikoura, J.

Frequency of hereditary nonpolyposis colorectal cancer: A prospective multicenter study in Finland. *Dis. Colon Rectum* **38**: 588-593, 1995.

Modrich, P. Mechanisms and biological effects of mismatch repair. *Ann. Rev. Genet.* **25**: 229-253, 1991.

Modrich, P. Mismatch repair, genetic stability, and cancer. *Science* **266**: 1959-1560, 1994.

Molenaar, M., van de Wetering, M., Oosterwegel, M., Peterson-Maduro, J., Godsave, S., Korinek, V., Roose, J., Destree, O., Clevers, H. XTcf-3 transcription factor mediates beta-catenin-induced axis formation in Xenopus embryos. *Cell* **86**: 391-399, 1996.

Moslein, G., Tester, D. J., Lindor, N. M., Honchel, R., Cunningham, J. M., French, A. J., Halling, K. C., Schwab, M., Goretzki, P., and Thibodeau, S. N. Microsatellite instability and mutation analysis of *hMSH2* and *hMLH1* in patients with sporadic, familial and hereditary colorectal cancer. *Hum. Mol. Genet.* **5**: 1245-1252, 1996.

Mullis, K. B. and Faloona, F. A. Specific synthesis of DNA in vitro via a polymerase-catalyzed chain reaction. *Methods Enzymol.* **155**: 335-350, 1987.

Nicolaides, N. C., Papadopoulos, N., Liu, B., Wei, Y. F., Carter, K. C., Ruben, S. M., Rosen, C. A., Haseltine, W. A., Fleischmann, R. D., Fraser, C. M., Adams, M. D., Venter, J. G., Dunlop, M. G., Hamilton, S. R., Peterson, G. M., de la Chapelle, A., Vogelstein, B., and Kinzler, K. W. Mutations of two PMS homologues in hereditary nonpolyposis colon cancer. *Nature* **371**: 75-80, 1994.

Nishisho, I., Nakamura, Y., Miyoshi, Y., Miki, Y., Ando, H., Horii, A., Koyama, K., Utsunomiya, J., Baba, S., and Hedge, P. Mutations of chromosome 5q21 genes in FAP and colorectal cancer patients. *Science* **253**: 665-669, 1991.

Palombo, F., Gallinari, P., Iaccarino, I., Lettieri, T., Hughes, M., D'Arrigo, A., Truong, O., Hsuan, J. J., and Jiricny, J. GTBP, a 160-kilodalton protein essential for mismatch-binding activity in human cells. *Science* **268**: 1912-1914, 1995.

Papadopoulos, N. and Lindblom, A. Molecular basis of HNPCC: Mutations of MMR genes. *Hum. Mutat.* **10**: 89-99, 1997.

Papadopoulos, N., Nicolaides, N. C., Wei, Y. F., Ruben, S. M., Carter, K. C., Rosen, C. A., Haseltine, W. A., Fleischmann, R. D., Fraser, C. M., Adams, M. D., Venter, J. G., Hamilton, S. R., Peterson, G. M., Watson, P., Lynch, H. T., Peltomaki, P., Mecklin, J.-P., de la Chapelle, A., Kinzler, K. W., and Vogelstein, B. Mutation of a mutL homolog in hereditary colon cancer. *Science* **263**: 1625-1629, 1994.

Parker, S. L., Tong, T., Bolden, S., and Wingo, P. A. Cancer statistics. *CA Cancer J. Clin.* **46**: 5-27, 1996.

Parsons, R., Li, G. M., Longley, M. J., Fang, W. H., Papadopoulos, N., Jen, J., de la Chapelle, A., Kinzler, K. W., Vogelstein, B., and Modrich, P. Hypermutability and mismatch repair deficiency in RER+ tumor cells. *Cell* **75**: 1227-1236, 1993.

Peltomaki, P., Aaltonen, L. A., Sistonen, P., Pylkkanen, L., Mecklin, J. P., Jarvinen, H., Green, J. S., Jass, J. R., Weber, J. L., Leach, F. S., Peterson, G. M., Hamilton, S. R., de la Chapelle, A., and Vogelstein, B. Genetic mapping of a locus predisposing to human colorectal cancer. *Science* **260**: 810-812, 1993a.

Peltomaki, P., Lothe, R. A., Aaltonen, L. A., Pylkkanen, L., Nystrom-Lahti, M., Seruca, R., David, L., Holm, R., Ryberg, D., Haugen, A., Brogger, A., Borresen, A.-L., and de la Chappelle, A. Microsatellite instability is associated with tumors that characterize the hereditary non-polyposis colorectal carcinoma syndrome. *Cancer Res.* **53**: 5853-5855, 1993b.

Platten, M., Giordano, M. J., Dirven, C. M., Gutmann, D. H., and Louis, D. N. Up-regulation of specific NF 1 gene transcripts in sporadic pilocytic astrocytomas. *Am. J. Pathol.* **149**: 621-627, 1996.

Prolla, T. A., Baker, S. M., Harris, A. C., Tsao, J. L., Yao, X., Bronner, C. E., Zheng, B., Gordon, M., Reneker, J., Arnheim, N., Shibata, D., Bradley, A., and Liskay, R. M. Tumour susceptibility and spontaneous mutation in mice deficient in *Mlh1*, *Pms1* and *Pms2* DNA mismatch repair. *Nat. Genet.* **18**: 276-279, 1998.

Purandare, S. M., Lanyon, W. G., and Connor, J. M. Characterisation of inherited and sporadic mutations in neurofibromatosis type-1. *Hum. Mol. Genet.* **3**: 1109-1115, 1994.

Rampino, N., Yamamoto, H., Ionov, Y., Li, Y., Sawai, H., Reed, J. C., and Perucho, M. Somatic frameshift mutations in the BAX gene in colon cancers of the microsatellite mutator phenotype. *Science* **275**: 967-969, 1997.

Reitmair, A. H., Redston, M., Cai, J. C., Chuang, T. C., Bjerknes, M., Cheng, H., Hay, K., Gallinger, S., Bapat, B., and Mak, T. W. Spontaneous intestinal carcinomas and skin neoplasms in Msh2-deficient mice. *Cancer Res.* **56**: 3842-3849, 1996.

Riccardi, V. M. Neurofibromatosis : Phenotype, Natural History, and Pathogenesis, 2nd edition. Baltimore: Johns Hopkins University Press, p. 498, 1992.

Ricciardone, M. D., Özçelik, T., Cevher, B., Özdağ, H., Tuncer, M., Gürgey, A., Uzunalimoğlu, Ö., Çetinkaya, H., Tanyeli, A., Erken, E., and Öztürk, M. Human *MLH1* deficiency predisposes to hematological malignancy and neurofibromatosis type 1. *Cancer Res.* **59**: 290-293, 1999.

Risinger, J. I., Umar, A., Boyd, J., Berchuck, A., Kunkel, T. A., and Barrett, J. C. Mutation of MSH3 in endometrial cancer and evidence for its functional role in heteroduplex repair. *Nat. Genet.* **14**: 102-105, 1996.

Rodenhiser, D. I., Andrews, J. D., Mancini, D. N., Jung, J. H., and Singh, S. M. Homonucleotide tracts, short repeats and CpG/CpNpG motifs are frequent sites for heterogeneous mutations in the neurofibromatosis type 1 (*NF1*) tumour-suppressor gene. *Mutat. Res.* **373**: 185-195, 1997.

Roest, P. A., Roberts, R. G., Sugino, S., van Ommen, G. J., and den Dunnen, J. T. Protein truncation test (PTT) for rapid detection of translation- terminating mutations. *Hum. Mol. Genet.* **2**: 1719-21, 1993.

Rubinfeld, B., Souza, B., Albert, I., Muller, O., Chamberlain, S. H., Masiarz, F. R., Munemitsu, S., Polakis, P. Association of the APC gene product with beta-catenin. *Science* **262**: 1731-1734, 1993.

Sawada, S., Florell, S., Purandare, S. M., Ota, M., Stephens, K., and Viskochil, D. Identification of *NF1* mutations in both alleles of a dermal neurofibroma. *Nat. Genet.* **14**: 110-112, 1996.

Schaaper, R. M. Base selection, proofreading, and mismatch repair during DNA replication in Escherichia coli. *J. Biol. Chem.* **268**: 23762-23765, 1993.

Scheffzek, K., Ahmadian, M. R., Wiesmuller, L., Kabsch, W., Stege, P., Schmitz, F., and Wittinghofer, A. Structural analysis of the GAP-related domain from neurofibromin and its implications. *Embo J.* **17**: 4313-4327, 1998.

Shen, M. H., Harper, P. S., and Upadhyaya, M. Molecular genetics of neurofibromatosis type 1 (*NF1*). *J. Med. Genet.* **33**: 2-17, 1996.

Skuse, G. R. and Cappione, A. J. RNA processing and clinical variability in neurofibromatosis type I (NF1). *Hum. Mol. Genet.* **6**: 1707-12, 1997.

Skuse, G. R., Cappione, A. J., Sowden, M., Metheny, L. J., and Smith, H. C. The neurofibromatosis type I messenger RNA undergoes base-modification RNA editing. *Nucleic Acids Res.* **24**: 478-485, 1996.

Smith, H. C. and Sowden, M. P. Base-modification mRNA editing through deamination--the good, the bad and the unregulated. *Trends Genet.* **12**: 418-424, 1996.

Sorensen, S. A., Mulvihill, J. J., and Nielsen, A. Long-term follow-up of von Recklinghausen neurofibromatosis: Survival and malignant neoplasms. *N. Engl. J. Med.* **314**: 1010-1015, 1986.

Strand, M., Prolla, T. A., Liskay, R. M., and Petes, T. D. Destabilization of tracts of simple repetitive DNA in yeast by mutations affecting DNA mismatch repair [published erratum appears in *Nature* **368**: 569, 1994]. *Nature* **365**: 274-276, 1993.

Souza, R. F., Appel, R., Yin, J., Wang, S., Smolinski, K. N., Abraham, J. M., Zou, T. T., Shi, Y. Q., Lei, J., Cottrell, J., Cymes, K., Biden, K., Simms, L., Leggett, B., Lynch, P. M., Frazier, M., Powell, S. M., Harpaz, N., Sugimura, H., Young, J., Meltzer, S. J. Microsatellite instability in the insulin-like growth factor II receptor gene in gastrointestinal tumours. [published erratum in *Nat Genet* **14**: 488, 1996]. *Nat Genet* **14**: 255-257, 1996.

Suzuki, H., Takahashi, K., Kubota, Y., and Shibahara, S. Molecular cloning of a cDNA coding for neurofibromatosis type 1 protein isoform lacking the domain related to ras GTPase-activating protein. *Biochem. Biophys. Res. Commun.* **187**: 984-90, 1992.

Suzuki, Y., Suzuki, H., Kayama, T., Yoshimoto, T., and Shibahara, S. Brain tumors predominantly express the neurofibromatosis type 1 gene transcripts containing

the 63 base insert in the region coding for GTPase activating protein-related domain. *Biochem. Biophys. Res. Commun.* **181**: 955-961, 1991.

Takahashi, K., Suzuki, H., Kayama, T., Suzuki, Y., Yoshimoto, T., Sasano, H., and Shibahara, S. Multiple transcripts of the neurofibromatosis type 1 gene in human brain and in brain tumours. *Clin. Sci. (Colch).* **87**: 481-485, 1994.

Tannegard P., Liu T., Weger A., Nordensgjold M., Lindblom A. Tumorigenesis in colorectal tumors from patients with hereditary non-polyposis colorectal cancer. *Hum. Genet.* **101:** 51-55, 1997.

Thibodeau, S. N., Bren, G., and Schaid, D. Microsatellite instability in cancer of the proximal colon. *Science* **260**: 816-819, 1993.

Thibodeau, S. N., French, A. J., Cunningham, J. M., Tester, D., Burgart, L. J., Roche, P. C., McDonnell, S. K., Schaid, D. J., Vockley, C. W., Michels, V. V., Farr, G. H., Jr., and O'Connell, M. J. Microsatellite instability in colorectal cancer: different mutator phenotypes and the principal involvement of *hMLH1*. *Cancer Res.* **58**: 1713-1718, 1998.

Tomlinson, I. P., Ilyas, M., and Bodmer, W. F. Allele loss occurs frequently at *hMLH1*, but rarely at *hMSH2*, in sporadic colorectal cancers with microsatellite instability. *Br. J. Cancer* **74**: 1514-1517, 1996.

Trinh, T. Q. and Sinden, R. R. Preferential DNA secondary structure mutagenesis in the lagging strand of replication in E. coli. *Nature* **352**: 544-547, 1991.

Umar, A., Buermeyer, A. B., Simon, J. A., Thomas, D. C., Clark, A. B., Liskay, R. M., and Kunkel, T. A. Requirement for PCNA in DNA mismatch repair at a step preceding DNA resynthesis. *Cell* **87**: 65-73, 1996.

Umar, A., Koi, M., Risinger, J. I., Glaab, W. E., Tindall, K. R., Kolodner, R. D., Boland, C. R., Barrett, J. C., and Kunkel, T. A. Correction of hypermutability, N-methyl-N'-nitro-N-nitrosoguanidine resistance, and defective DNA mismatch repair by introducing chromosome 2 into human tumor cells with mutations in MSH2 and MSH6. *Cancer Res.* **57**: 3949-2955, 1997.

Upadhyaya, M., Osborn, M. J., Maynard, J., Kim, M. R., Tamanoi, F., and Cooper, D. N. Mutational and functional analysis of the neurofibromatosis type 1 (*NF1*) gene. *Hum. Genet.* **99**: 88-92, 1997.

Valero, M. C., Velasco, E., Moreno, F., and Hernandez-Chico, C. Characterization of four mutations in the neurofibromatosis type 1 gene by denaturing gradient gel electrophoresis (DGGE). *Hum. Mol. Genet.* **3**: 639-641, 1994.

van der Luijt, R. B., Tops, C. M., Khan, P. M., van der Klift, H. M., Breukel, C., van Leeuwen-Cornelisse, I. S., Dauwerse, H. G., Beverstock, G. C., van Noort, E., Snel, P., *et al.* Molecular, cytogenetic, and phenotypic studies of a constitutional reciprocal translocation t(5;10)(q22;q25) responsible for familial adenomatous polyposis in a Dutch pedigree. *Genes Chromosomes Cancer* **13**: 192-202, 1995.

van Tuinen, P., Rich, D. C., Summers, K. M., and Ledbetter, D. H. Regional mapping panel for human chromosome 17: application to neurofibromatosis type 1. *Genomics* **1**: 374-81, 1987.

Viskochil, D., Buchberg, A. M., Xu, G., Cawthon, R. M., Stevens, J., Wolff, R. K., Culver, M., Carey, J. C., Copeland, N. G., Jenkins, N. A., and *et al.* Deletions and a translocation interrupt a cloned gene at the neurofibromatosis type 1 locus. *Cell* **62**: 187-92, 1990.

Wallace, M. R., Marchuk, D. A., Andersen, L. B., Letcher, R., Odeh, H. M., Saulino, A. M., Fountain, J. W., Brereton, A., Nicholson, J., Mitchell, A. L., Brownstein, B. H., and Collins, F. S. Type 1 neurofibromatosis gene: identification of a large transcript disrupted in three NF1 patients [published erratum appears in *Science* **250**: 1749, 1990]. *Science* **249**: 181-186, 1990.

Wang, Q., Lasset, C., Desseigne, F., Frappaz, D., Bergeron, C., Navarro, C., Ruano, E., Puisieux, A. Neurofibromatosis and early onset of cancers in *hMLH1*-deficient children. *Cancer Res* **59**: 294-297, 1999.

Watson, P., Vasen, H. F., Mecklin, J. P., Jarvinen, H., and Lynch, H. T. The risk of endometrial cancer in hereditary nonpolyposis colorectal cancer. *Am. J. Med.* **96**: 516-20, 1994.

White, M. B., Carvalho, M., Derse, D., O'Brien, S. J., and Dean, M. Detecting single base substitutions as heteroduplex polymorphisms. *Genomics* **12**: 301-6, 1992.

Wierdl, M., Greene, C. N., Datta, A., Jinks-Robertson, S., and Petes, T. D. Destabilization of simple repetitive DNA sequences by transcription in yeast. *Genetics* **143**: 713-721, 1996.

Wolfe, K. H., Sharp, P. M., and Li, W. H. Mutation rates differ among regions of the mammalian genome. *Nature* **337**: 283-285, 1989.

Xu, G. F., O'Connell, P., Viskochil, D., Cawthon, R., Robertson, M., Culver, M., Dunn, D., Stevens, J., Gesteland, R., White, R., and Weiss, R. The neurofibromatosis type 1 gene encodes a protein related to GAP. *Cell* **62**: 599-608, 1990.

Xu, G., O'Connell, P., Stevens, J., and White, R. Characterization of human adenylate kinase 3 (AK3) cDNA and mapping of the AK3 pseudogene to an intron of the *NF1* gene. *Genomics* **13**: 537-542, 1992.

Yamamoto, H., Sawai, H., Weber, T. K., Rodriguez-Bigas, M. A., and Perucho, M. Somatic frameshift mutations in DNA mismatch repair and proapoptosis genes in hereditary nonpolyposis colorectal cancer. *Cancer Res.* **58**: 997-1003, 1998.

Zoller, M., Rembeck, B., Akesson, H. O., and Angervall, L. Life expectancy, mortality and prognostic factors in neurofibromatosis type 1: A twelve-year follow-up of an epidemiological study in Goteborg, Sweden. *Acta. Derm. Venereol.* **75**: 136-140, 1995.